Foundation and Material Configurations:

Foundation and material configurations are summarized in Table 3.

Bearing capacity is evaluated for two extreme foundation widths (B); the shortest east-west dimension on the south edge of the building (B = 88 feet), and the longest east-west dimension (shown on Figure 5) through the shield building and the auxiliary building (B = 160 feet). Rock and soil properties (c', φ', γ) are determined by an arithmetic average weighted by thickness of the underlying strata.

Rock-only bearing capacity is evaluated using a weighted average with properties of the Key Largo and Fort Thompson formations only. An additional case using weighted averages to a depth of 2B, including soil layers, is evaluated for rock and soil together in local shear failure evaluation. Soil-only bearing capacity is evaluated using weighted averages of the upper Tamiami, lower Tamiami, and Peace River to a depth of 2B.

Properties for rock are varied between assumptions of very slightly fractured rock (fracture density = 1, FD1), slightly to moderately fractured rock (FD4), and lower bound rock (as discussed in the revised response to RAI 02.05.04-09, provided here, and included in FSAR Table 2.5.4-221, which is updated in the revised response to RAI 02.05.04-09). Soil is varied between best estimate properties and lower bound properties. For lower bound properties in soil, the upper Tamiami is reduced to the properties in FSAR Table 2.5.4-221 while lower Tamiami and Peace River properties remain as best estimate properties. It is unrealistic to assign lower bound properties to all layers, so the upper Tamiami was reduced, as it is the bearing layer in soil-only calculations.

To obtain static bearing capacity according to Hoek-Brown methodology, Table 1 from Reference 9 is followed (see Table 2). The rock mass at Units 6 & 7 is tightly interlocking undisturbed carbonate rock and is classified as very good quality rock. The material parameters m and s (Reference 9) are interpolated accordingly into the methodology described in Reference 3. To be conservative, the average UCS value of the two rock layers is adopted, this is approximately equal to 17 megapascals (MPa). Foundation configuration is not considered in Hoek-Brown methodology.

Punching failure also uses the average UCS of the Key Largo and Fort Thompson formations. This failure is determined for the two foundation configurations (88 feet and 160 feet) instead of the two rock strengths (FD4 and FD1) since UCS is not determined for FD4 conditions.

In SLOPE/W, a case is considered where zones representing open discontinuities are placed beneath and to the side of the NI to represent zones of FD4 material as shown in Figure 5. This case is unrealistic because joints in FD4 rock are only moderately open, but is presented to show an extreme case that still meets the bearing demand criteria.

In SLOPE/W, the extreme case of simulated FD4 zones is evaluated differently than the other SLOPE/W cases, by finding the factor of safety when the bearing demand pressure of 8.9 ksf is applied instead of finding the allowable bearing capacity for a prescribed factor of safety. The following failures are found for configurations with and without simulated FD4 zones (Figures 6 and 7).

The factor of safety with simulated FD4 zones (FS = 6.2) is almost half of the factor of safety with no FD4 zones (FS = 11.6). This low factor of safety is still more than double the required FS=3.0

In PLAXIS 2D, the beam tension failure is checked for the required bearing demand (8.9 ksf) as well as three times the required bearing demand (26.7 ksf). In Figures 8 and 9, points in tension are shown with black circles. As evident in both cases, there are minimal black circles, i.e., no tensile failure is observed.

If the load is increased high enough, the failure pattern observed from PLAXIS 2D (Figure 4)resembles the one obtained from SLOPE/W. PLAXIS 2D also shows that at the interface of Fort Thompson and Upper Tamiami formations, series of points go into the plastic zone (Mohr Coulomb shear failure). These points are in addition to the typical general shear failure shape, and are attributed to the strength and stiffness contrast between the two formations. The plastic points at the Fort Thompson and Upper Tamiami formations do not preclude the general failure pattern from forming all the way to the surface. In other words, series of points at this interface experience shear failure while the general shear failure is also fully developed. Nevertheless, the load to reach this type of failure is at least 20 times the foundation bearing demand.

Figure 5 Estimated Locations of FD4 Zones
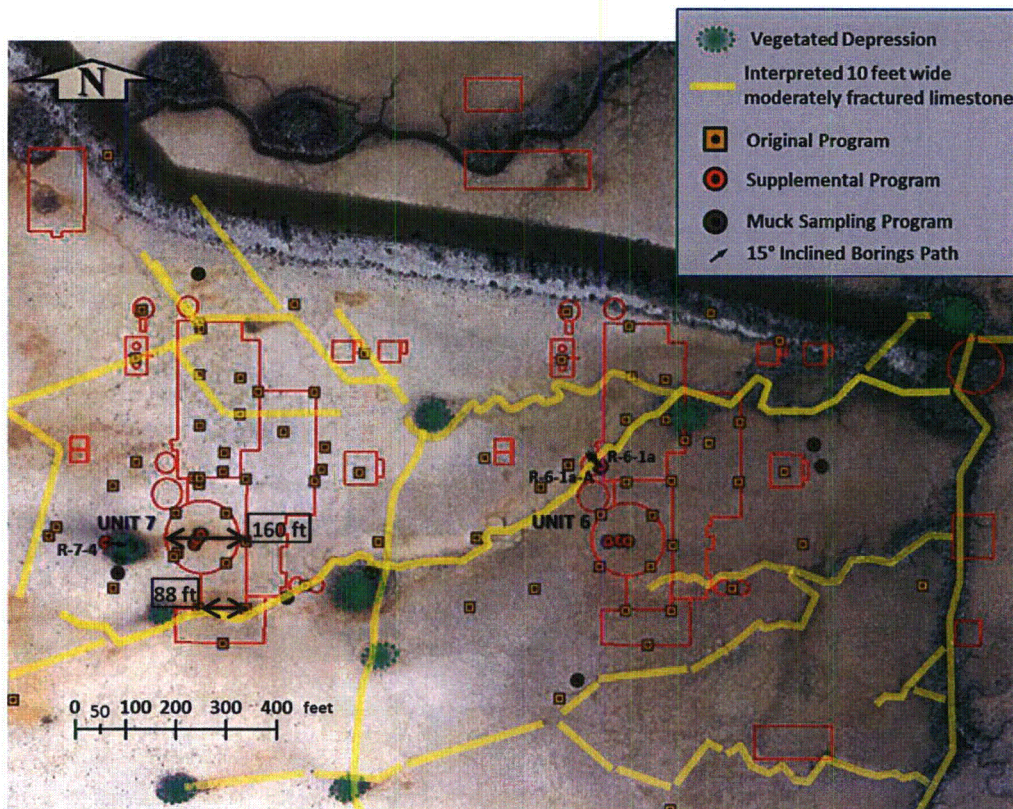
Google earth image 1/30/2005 U.S. Geological Survey

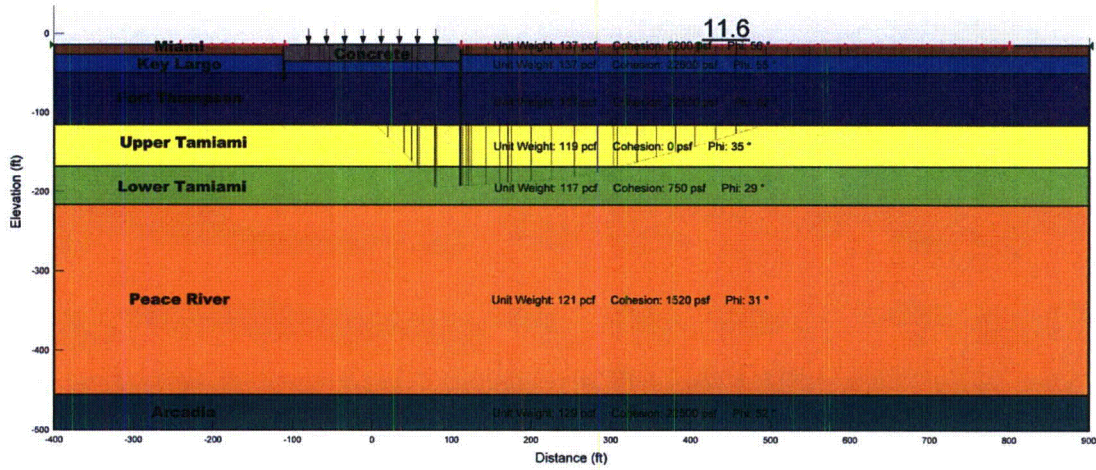**Figure 6 No Discontinuities, 1x Required Bearing Demand**

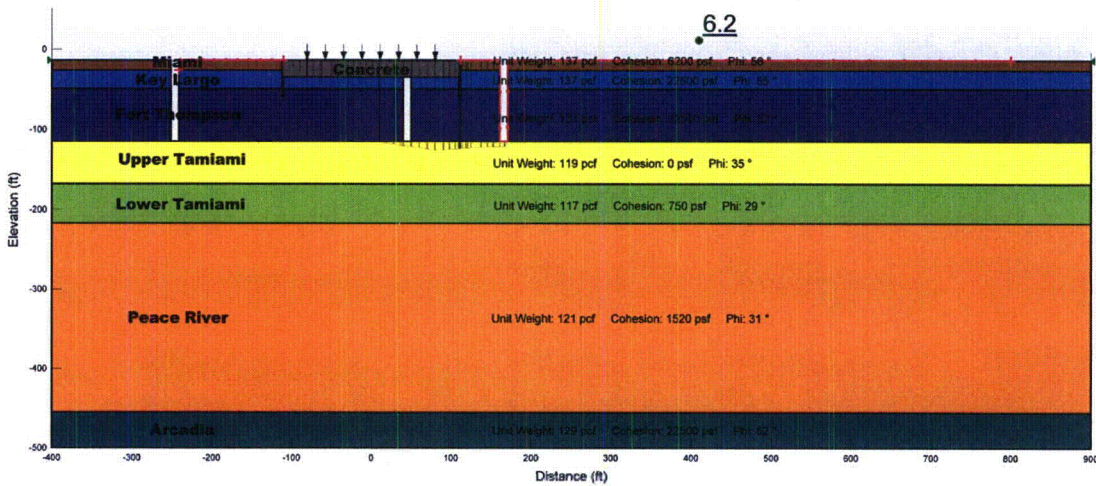**Figure 7 Simulated Discontinuities, 1x Required Bearing Demand**

Figure 8 Plastic Deformation from PLAXIS 2D Analysis, 1x Required Bearing Demand
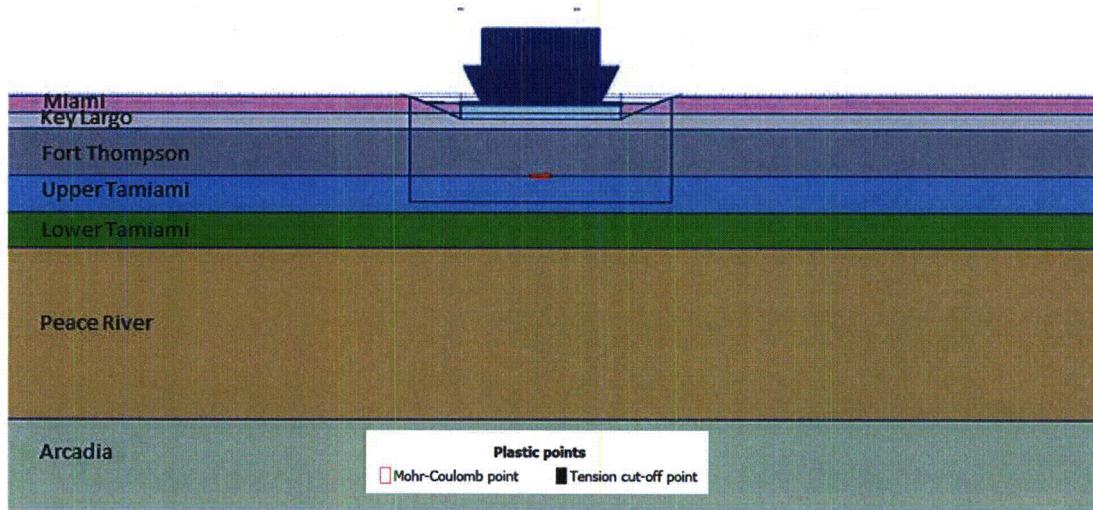

Figure 9 Plastic Deformation from PLAXIS 2D Analysis, 3x Required Bearing Demand
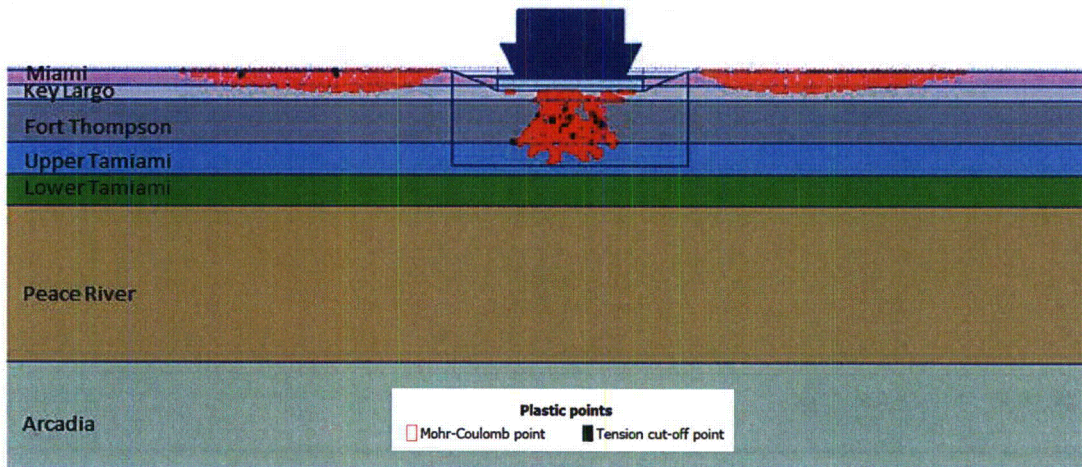
Table 2

Hoek-Brown Material Constants

Table 1 : Approximate relationship between rock mass quality and material constants						
Disturbed rock mass m and s values				undisturbed rock mass m and s values		
EMPIRICAL FAILURE CRITERION $\sigma_1' = \sigma_3' + \sqrt{m\sigma_c\sigma_3' + s\sigma_c^2}$ σ_1' = major principal effective stress σ_3' = minor principal effective stress σ_c = uniaxial compressive strength of intact rock, and m and s are empirical constants.		**CARBONATE ROCKS WITH WELL DEVELOPED CRYSTAL CLEAVAGE** *dolomite, limestone and marble*	**LITHIFIED ARGILLACEOUS ROCKS** *mudstone, siltstone, shale and slate (normal to cleavage)*	**ARENACEOUS ROCKS WITH STRONG CRYSTALS AND POORLY DEVELOPED CRYSTAL CLEAVAGE** *sandstone and quartzite*	**FINE GRAINED POLYMINERALLIC IGNEOUS CRYSTALLINE ROCKS** *andesite, dolerite, diabase and rhyolite*	**COARSE GRAINED POLYMINERALLIC IGNEOUS & METAMORPHIC CRYSTAL-LINE ROCKS** – *amphibolite, gabbro gneiss, granite, norite, quartz-diorite*
INTACT ROCK SAMPLES *Laboratory size specimens free* *from discontinuities* CSIR rating: RMR = 100 NGI rating: Q = 500	m s m s	7.00 1.00 *7.00* *1.00*	10.00 1.00 *10.00* *1.00*	15.00 1.00 *15.00* *1.00*	17.00 1.00 *17.00* *1.00*	25.00 1.00 *25.00* *1.00*
VERY GOOD QUALITY ROCK MASS *Tightly interlocking undisturbed rock* *with unweathered joints at 1 to 3m.* CSIR rating: RMR = 85 NGI rating: Q = 100	m s m s	2.40 0.082 *4.10* *0.189*	3.43 0.082 *5.85* *0.189*	5.14 0.082 *8.78* *0.189*	5.82 0.082 *9.95* *0.189*	8.56 0.082 *14.63* *0.189*
GOOD QUALITY ROCK MASS *Fresh to slightly weathered rock, slightly* *disturbed with joints at 1 to 3m.* CSIR rating: RMR = 65 NGI rating: Q = 10	m s m s	0.575 0.00293 *2.006* *0.0205*	0.821 0.00293 *2.865* *0.0205*	1.231 0.00293 *4.298* *0.0205*	1.395 0.00293 *4.871* *0.0205*	2.052 0.00293 *7.163* *0.0205*
FAIR QUALITY ROCK MASS *Several sets of moderately weathered* *joints spaced at 0.3 to 1m.* CSIR rating: RMR = 44 NGI rating: Q = 1	m s m s	0.128 0.00009 *0.947* *0.00198*	0.183 0.00009 *1.353* *0.00198*	0.275 0.00009 *2.030* *0.00198*	0.311 0.00009 *2.301* *0.00198*	0.458 0.00009 *3.383* *0.00198*
POOR QUALITY ROCK MASS *Numerous weathered joints at 30-500mm,* *some gouge. Clean compacted waste rock* CSIR rating: RMR = 23 NGI rating: Q = 0.1	m s m s	0.029 0.000003 *0.447* *0.00019*	0.041 0.000003 *0.639* *0.00019*	0.061 0.000003 *0.959* *0.00019*	0.069 0.000003 *1.087* *0.00019*	0.102 0.000003 *1.598* *0.00019*
VERY POOR QUALITY ROCK MASS *Numerous heavily weathered joints spaced* *<50mm with gouge. Waste rock with fines.* CSIR rating: RMR = 3 NGI rating: Q = 0.01	m s m s	0.007 0.0000001 *0.219* *0.00002*	0.010 0.0000001 *0.313* *0.00002*	0.015 0.0000001 *0.469* *0.00002*	0.017 0.0000001 *0.532* *0.00002*	0.025 0.0000001 *0.782* *0.00002*

Source: Reference 9

Table 3
Foundation and Material Configurations for Bearing Capacity Analysis

Evaluation Method	Foundation Width, B (feet)	Properties[1]	Local Shear Failure	Hoek-Brown [2]	Punching Failure[3]	Beam Tension Failure
Rock-Only Hand Calculation	88	FD1 Rock	X	X	X	−
Rock-Only Hand Calculation	160	FD1 Rock	X	X	X	−
Rock-Only Hand Calculation	88	FD4 Rock	X	−	−	−
Rock-Only Hand Calculation	160	FD4 Rock	X	−	−	−
Rock-Only Hand Calculation	88	LB FD4 Rock	X	−	−	−
Rock-Only Hand Calculation	160	LB FD4 Rock	X	−	−	−
Rock & Soil Hand Calculation	88	FD4 Rock & BE Soil	X	−	−	−
Rock & Soil Hand Calculation	160	FD4 Rock & BE Soil	X	−	−	−
Rock & Soil Hand Calculation	88	LB FD4 Rock & BE Soil	X	−	−	−
Rock & Soil Hand Calculation	160	LB FD4 Rock & BE Soil	X	−	−	−
Soil-Only Hand Calculation	88	BE Soil	X	−	−	−
Soil-Only Hand Calculation	160	BE Soil	X	−	−	−
Soil-Only Hand Calculation	88	LB Soil	X	−	−	−
Soil-Only Hand Calculation	160	LB Soil	X	−	−	−
SLOPE/W	88	FD1 Rock & BE Soil	X	−	−	−
SLOPE/W	160	FD1 Rock & BE Soil	X	−	−	−
SLOPE/W	160	LB FD4 Rock & LB Soil	X	−	−	−
SLOPE/W	160	FD1 Rock with open joints	X	−	−	−
PLAXIS 2D	160	FD1 Rock & BE Soil	X	−	−	X

[1] LB Soil includes LB properties of upper Tamiami and BE properties for lower Tamiami and Peace River
[2] Hoek-Brown methodology is dimension independent
[3] Punching failure is based on lowest average UCS of rock layers
BE = Best Estimate
LB = Lower Bound, as defined in the revised response to RAI 02.05.04-09

Summary and Recommendation:

Ultimate and allowable bearing capacities for the failures marked in Table 2 are presented in Table 3, with the exception of two cases. The SLOPE/W model with simulated FD4 zones and the PLAXIS 2D model do not produce allowable bearing capacities to populate Table 3. They are included for visual inspection of the failure surface.

For static analyses, the lowest allowable bearing capacity of 39 ksf results from the Lower Bound configuration in SLOPE/W (Table 3). This static bearing capacity is acceptable according to the 8.9 ksf static bearing demand required by the AP1000 DCD.

For dynamic analyses, the minimum allowable bearing capacity using Soubra's methodology (Reference 4) is 43 ksf, resulting from the soil-only analysis using lower bound properties for the upper Tamiami layer. This dynamic bearing capacity is acceptable according to the 35 ksf bearing demand required by the DCD.

Recommended static bearing capacity at Units 6 & 7 is 39 ksf and recommended dynamic bearing capacity is 43 ksf.

Table 4

Summary of Calculated Bearing Capacities (ksf)

Evaluation Method	Foundation Width, B (ft)	Properties	Local Shear Failure				Hoek-Brown[1]		Punching[2]	
			Static, q_{ULT}	Static, q_{ALL}	Dynamic, q_{ULT}	Dynamic, q_{ALL}	Static, q_{ULT}	Static, q_{ALL}	Static, q_{ULT}	Static, q_{ALL}
Rock-Only Hand Calculation	88	FD1 Rock	2,623	874	3,701	1,851	1629	543	408	136
Rock-Only Hand Calculation	160	FD1 Rock	3,603	1,201	4,640	2,320			273	91
Rock-Only Hand Calculation	88	FD4 Rock	1,790	597	2,104	1,052	–	–	–	–
Rock-Only Hand Calculation	160	FD4 Rock	2,771	924	2,999	1,500	–	–	–	–
Rock-Only Hand Calculation	88	LB FD4 Rock	1,063	354	1,411	706	–	–	–	–
Rock-Only Hand Calculation	160	LB FD4 Rock	1,748	583	2,214	1,107	–	–	–	–
Rock & Soil Hand Calculation	88	FD4 Rock & BE Soil	386	129	658	329	–	–	–	–
Rock & Soil Hand Calculation	160	FD4 Rock & BE Soil	329	110	401	201	–	–	–	–
Rock & Soil Hand Calculation	88	LB FD4 Rock & BE Soil	279	93	485	243	–	–	–	–
Rock & Soil Hand Calculation	160	LB FD4 Rock & BE Soil	280	93	339	170	–	–	–	–
Soil-Only Hand Calculation	88	BE Soil	165	55	87	44	–	–	–	–
Soil-Only Hand Calculation	160	BE Soil	251	84	138	69	–	–	–	–
Soil-Only Hand Calculation	88	LB Soil	157	52	87	43	–	–	–	–
Soil-Only Hand Calculation	160	LB Soil	244	81	138	69	–	–	–	–
SLOPE/W	88	FD1 Rock & BE Soil	–	81	–	–	–	–	–	–
SLOPE/W	160	FD1 Rock & BE Soil	–	51	–	–	–	–	–	–
SLOPE/W	160	LB FD4 Rock & LB Soil	–	39	–	–	–	–	–	–
Minimum/Recommended			157	39	87	43	694	231	273	91

[1] LB Soil includes LB properties of upper Tamiami and BE properties for lower Tamiami and Peace River
[2] Hoek-Brown methodology is dimension independent
[3] Punching failure is based on lowest average UCS of rock layers
q_{ULT} = ultimate bearing capacity
q_{ALL} = allowable bearing capacity
BE = Best Estimate
LB = Lower Bound as defined in the revised response to RAI 02.05.04-09

Part B

Recommended bearing capacity does not implement UCS. UCS is only used in calculation of Hoek-Brown bearing capacity and tensile strength as the average of Key Largo and Fort Thompson data.

Values for UCS are discussed in the revised response to RAI 02.05.04-04. In this RAI response, the average values for each rock layer are updated in Tables 2.5.4-207 and 2.5.4-209 to include data from the supplemental investigation. These averages are determined arithmetically.

This response is PLANT SPECIFIC.

References:

1.   Bowles, J. E., *Foundation Analysis and Design*, The McGraw-Hill Companies, Inc., 1997, pp. 219-228.

2.   USACE, *Rock Foundations*, Engineering Manual EM 1110-1-2908, Ch. 6, 1994.

3.   Carter, J.P. and Kulhawy, F.H., *Analysis and Design of Drilled Shaft Foundations Socketed into Rock*, Report EL-5918, Electric Power Research Institute, Palo Alto, CA, pp. 3-2 through 3-6, 1988.

4.   Soubra, A. H., *Upper-Bound Solutions for Bearing Capacity of Foundations*, J. Geotechnical and Geoenvironmental Engineering, January, V. 125, No. 1, p. 59, 1999.

5.   Hoek, E., C. Carranza-Torres, and B. Corkum, *Generalized Hoek-Brown Failure Criterion - 2002 Edition,* 5th North American Rock Mechanics, 2002.

6.   Wyllie, D., *Foundations on Rock*, 2nd Edition, pp 143 and 144, 1999.

7.   Prakoso, W.A. and F.H. Kulhawy, *Capacity of Foundations on Discontinuous Rock*, Golden Rocks 2006 (Proceedings of the 41st US Symposium of Rock Mechanics), Ed. DP Yale et al., Paper 06-972, page 3-2, 2006.

8.   GEO-SLOPE International Ltd., *Stability Modeling with SLOPE/W 2007 Version: An Engineering Methodology*, Fourth Edition, p. 54, February 2010.

9.   Hoek, E, and E.T. Brown, "The Hoek-Brown Failure Criterion – a 1988 Update," Proceedings of the 15th Canadian Rock Mechanics Symposium, Toronto, 1988

ASSOCIATED COLA REVISIONS:

FSAR Subsection 2.5.4.10.2 will be revised in a future revision as follows:

Application of classical bearing capacity hand calculations, such as Vesic's methodology (Reference 225) or methods outlined in Reference 272, to obtain the bearing capacity of the foundation media underlying the NI is not straightforward due to the strength difference between rock and soil formations as seen in Table 2.5.4-209. Therefore, simplified configurations are assumed to calculate bearing capacity on:

1. **Rock only, using Hoek-Brown's methodology (described in Reference 314), local shear failure for rock (References 272 and 316), and punching failure (Reference 272).**

2. **Rock and soil together, using local shear failure for rock (Reference 272).**

3. **Soil only, using local shear failure from Vesic's methodology (described in Reference 225), as if the NI basemat was founded on the upper Tamiami layer.**

Due to the predominantly massive nature of rock layers at Units 6 & 7, as well as the rough condition of observed discontinuities, jointed rock failure modes are not considered in this bearing capacity analysis. Without open joints, stress is permitted to transmit continuously through the foundation media promoting a general shear failure mode.

The ultimate bearing capacity, q_{ult}, of a foundation **on soil** is calculated using **Vesic's methodology for general shear failure from** Reference 225:

$$q_{ult} = c\, N_c\, \zeta_c + q\, N_q\, \zeta_q + 0.5\, \gamma'\, B\, N_\gamma \zeta_\gamma \qquad \text{Equation 2.5.4-14}$$

~~Category I seismic structures bear on lean concrete placed on the rock of Key Largo Limestone (Stratum 3).~~ For foundations bearing on rock, Reference**s** 272 **and 316** equations ~~is used~~ calculate bearing capacity **from general shear failure**.

Using Reference 272, the ultimate bearing capacity (q_{ult}) formula for a footing on weak rocks with little fracturing is calculated as:

$$q_{ult} = c\, N_c\, C_{f1} + \gamma\, D_f\, N_q + 0.5\gamma\, B\, N_\gamma C_{f2} \qquad \text{Equation 2.5.4-15}$$

Where,

c = rock mass cohesion
γD_f = effective overburden pressure at base of foundation
γ = effective unit weight of rock
D_f = depth from ground surface to base of foundation
B = width of foundation
N_c, N_q, and N_γ are bearing capacity factors for rock

Cf1 and Cf2 are shape factors that replace the ζ shape factor in Equation 2.5.4-14.

From Table 5.4 of Reference 272,

Cf1 = Cf2 = 1.0 for L/B>6 strip foundation	Equation 2.5.4-16a
Cf1 = 1.12, Cf2 = 0.9 for L/B=2	Equation 2.5.4-16b
Cf1 = 1.05, Cf2 = 0.95 for L/B=5	Equation 2.5.4-16c
Cf1 = 1.25, Cf2 = 0.85 for square foundation	Equation 2.5.4-16d
Cf1 = 1.2, Cf2 = 0.7 for circular foundation	Equation 2.5.4-16e

Where,

L = length of footing

From Equation 5.8 of Reference 272,

$N\varphi = \tan2(45+\varphi/2)$	Equation 2.5.4-17
$Nc = 2 N \varphi 0.5 (N\varphi+1)$	Equation 2.5.4-18
$N\gamma = 0.5 N\varphi0.5(N2\varphi-1)$	Equation 2.5.4-19
$Nq = N \varphi 2$	Equation 2.5.4-20

Equations 2.5.4-14 and 2.5.4-15 can be simplified to a local shear failure mode:

$$q_{ult} = c\, N_c\, \zeta_c + 0.5\, \gamma\, B\, N_\gamma\, \zeta_\gamma \qquad\qquad \text{Equation 2.5.4-14a}$$

$$q_{ult} = cN_cC_{f1} + 0.5\, \gamma\, B\, N_\gamma\, C_{f2} \qquad\qquad \text{Equation 2.5.4-15a}$$

This simplification is conservative because it neglects the contribution of the second ~~two terms.~~ relating to surcharge resistance. Therefore, local shear failure evaluation is used in bearing capacity analysis instead of the general shear failure assumption.

~~Since there were no laboratory test results available to derive rock mass cohesion or friction angle for Miami Limestone, a generic value was used from Reference 272. For limestones with 10 to 20 mm clay infillings, c = 2.3 ksf and φ = 14°. Using Equation 2.5.4-215a gives an allowable bearing capacity of 5.8 ksf, including a factor of safety of 3.~~

~~Alternatively, an allowable bearing capacity of not more than 20 percent of the unconfined compressive strength (U) of the rock can be used, according to Reference 221. For the Miami Limestone, a U of 200 psi is given in Table 2.5.4-209. Twenty percent of this strength is 40 psi (5.76 ksf). The results of the two methods compare favorably.~~

~~The foundation bearing capacities of the Category 1 seismic structures are considered similarly. The design U for the Key Largo Limestone is 1.5 ksi from Table 2.5.4-209 with 20 percent of 1.5 ksi = 300 psi ~ 43 ksf. This allowable capacity compares favorably to the value of 54.5 ksf which is calculated using Equation 2.5.4-15a (conservatively assuming a friction angle that is the same as for the Miami Limestone = 14° and a cohesion of 10 percent of the U, i.e., 21.6 ksf); the lower value of 43 ksf is recommended.~~

In addition to Equation 2.5.4-15a for a local shear failure in rock, the Hoek-Brown methodology considers the strength criterion for jointed rock masses to calculate ultimate bearing capacity. The Hoek-Brown methodology assumes a strip footing, but does not take foundation dimensions into account. Instead, the method relies on

rock descriptions and unconfined compressive strength, shown in Equation 3-6 of Reference 314:

$$q_{ult} = \left[\sqrt{s} + m\right] \times U \qquad \text{Equation 2.5.4-20a}$$

Where,

> q_{ult} = ultimate bearing capacity,
> U = unconfined compressive strength of a rock mass, and
> m and s = empirically-determined strength parameters according to rock type, and rock condition, listed in Reference 274.

Punching failure describes a case where the overlying rock layers fail in shear on all sides of the foundation due to the concentrated force on thin rock layers. This failure is also applicable to bearing capacity analysis of Units 6 & 7. Punching failure bearing capacity is defined as the rock layer shear strength multiplied by the shearing surface area. The shearing surface area is equal to the loading perimeter multiplied by the thickness of the rock layer.

$$q_{ult} = \frac{U}{2} * (2B + 2L) * H / (B * L) \qquad \text{Equation 2.5.4-20a}$$

Where,

> q_{ult} = ultimate bearing capacity,
> U = unconfined compressive strength of a rock mass,
> B = width of foundation,
> L = length of foundation, and
> H = thickness of Key Largo plus Fort Thompson beneath the bearing surface (Table 2.5.4-209).

To adequately consider both rock and soil formations, bearing capacity is additionally obtained using SLOPE/W software (limit-equilibrium method) and justified using PLAXIS 2D. In SLOPE/W the foundation bearing demand is increased until the desired factor of safety is observed (FS = 3.0). Allowable bearing capacity is obtained at FS = 3.0. When the load is further increased, the ultimate failure surface is observed at FS = 1.0. These conditions are presented in Figures 2.5.4-256 and 2.5.4-257. These surfaces are checked with PLAXIS 2D (finite element method) to obtain a unique solution independent of the prescribed failure surfaces in SLOPE/W.

PLAXIS 2D is used to verify the validity of failure surfaces from SLOPE/W using the unique solution found from increasing the bearing demand to failure. As seen in a plot of plastic points (i.e., points reaching Mohr-Coulomb failure), this unique surface becomes evident (Figure 2.5.4-268). This is the same depth reached by the prescribed failure surface from SLOPE/W (Figures 2.5.4-256 and 2.5.4-257).

The PLAXIS 2D model is also used to check for beam tension failure. The tension cutoff for the rock layers (i.e., tensile strength of rock) is determined according to equation 3.20 in Reference 272.

$$\sigma_t = 0.5\,\sigma_u\,(m - \sqrt{m^2 + 4s}) \hspace{3cm} \textbf{Equation 2.5.4-20b}$$

In PLAXIS 2D, the beam tension failure is checked for the required bearing demand (8.9 ksf) as well as three times the required bearing demand (26.7 ksf). In Figures 2.5.4-266 and 2.5.4-267, points in tension are shown with black circles. As evident in both cases, there are minimal black circles, i.e., no significant tensile failure, is observed, even for loads three times the required bearing demand.

Bearing capacity is evaluated for two extreme foundation widths (B): the shortest east-west dimension on the south edge of the building (B = 88 feet) and the longest east-west dimension through the shield building and the auxiliary building (B = 160 feet). Rock and soil properties (c', φ', γ) are determined by an arithmetic average weighted by thickness of the underlying strata (Table 2.5.4-209). These properties are determined for the following cases:

1.   Rock-only bearing capacity is evaluated using a weighted average with properties of the Key Largo and Fort Thompson formations only.

2.   Soil and rock together uses weighted averages to a depth of 2B, including soil layers.

3.   Soil-only bearing capacity is evaluated using weighted averages of the upper Tamiami, lower Tamiami, and Peace River to a depth of 2B.

Properties for rock are varied between assumptions of very slightly fractured rock (fracture density of = 1, FD1), slightly to moderately fractured rock (FD4), and lower bound rock (Table 2.5.4-221).

Soil is varied between best estimate properties and lower bound properties. For lower bound properties in soil, the upper Tamiami is reduced to the properties in Table 2.5.4-221 while lower Tamiami and Peace River properties remain as best estimate properties. It is unrealistic to assign lower bound properties to all layers, so the upper Tamiami was reduced as it is the bearing layer in soil-only calculations.

To obtain static bearing capacity according to Hoek-Brown methodology, material properties are estimated from Reference 319. The rock mass at Units 6 & 7 is tightly interlocking undisturbed carbonate rock, classified as very good quality. These material properties are used in Hoek-Brown bearing capacity and calculation of tensile strength for the beam tension failure check in PLAXIS 2D. The average UCS value of the two rock layers is adopted.

Punching failure also uses the average UCS of the Key Largo and Fort Thompson formations. This failure is determined for the two foundation configurations (88 feet and 160 feet).

In SLOPE/W, a case is considered where zones representing open discontinuities are placed beneath and to the side of the NI to represent zones of FD4 material as shown in Figure 2.5.4-254. This case is unrealistic because joints in FD4 rock are only moderately open, but the comparison to no simulated joints is presented in Figures 2.5.4-258 and 2.5.4-259.

Foundation bearing capacities are calculated using ~~the average material properties in Table 2.5.4-209 and~~ Equations 2.5.4-14**a, 2.5.4-15a and 2.5.4-16a** through 2.5.4-20**b**. A summary of the **cases evaluated and** allowable bearing capacities (using FOS = 3.0) of Seismic Category I structures (nuclear island) is given in Table 2.5.4-217. Analysis results show that for the Seismic Category I structures (including both units), the **minimum** allowable static bearing capacity is ~~43~~**39** ksf **from the lower bound SLOPE/W analysis**, which greatly exceeds the ~~anticipated~~ average required bearing capacity of 8.9 ksf specified in the DCD.

~~The above bearing capacity formulation is based on the assumption that the strata within the zone of foundation deformation are uniform with depth in terms of shear strength properties. While recognizing that the site strata are interlayered, the properties of the soil and rock are conservatively selected to provide for a representative bearing capacity.~~

FSAR Subsection 2.5.4.10.2.1 will be revised in a future COLA revision as follows:

2.5.4.10.2.1   Dynamic Bearing Capacity

Dynamic bearing capacity is determined using Soubra's bearing capacity factors (Reference 315), N_{cE} and $N_{\gamma E}$, in Equations 2.5.4-14a and 2.5.4-15a, replacing N_c and N_γ, respectively. These factors are chosen from Soubra's Tables 6 and 8 based on horizontal acceleration K_H = 0.1g and the friction angle according to the foundation media rounded down to the nearest 5.

The maximum dynamic bearing capacity required is 35 ksf (DCD). This total load includes normal loading plus seismic conditions with a 0.3g peak ground acceleration, which greatly exceeds the seismicity in Florida. Using the calculated allowable bearing capacity of 43 ksf for rock and lean concrete overlying the rock, this condition is satisfied even with the 0.3g peak ground acceleration.

Note that for concrete, no guidance is given in ACI 349-06 (Reference 273) for increasing or decreasing the design bearing strength for dynamic loading.

FSAR Subsection 2.5.4.11 will be revised in a future revision as follows:

2.5.4.11   Design Criteria and References

Table 2.5.4-217 contains calculated **allowable** bearing capacities, both static and dynamic, for Units 6 & 7 Seismic Category I structures. In the case of static bearing capacity, a minimum FOS = 3.0 is ~~applied against the calculated ultimate bearing capacity in evaluating the~~ **used to evaluate allowable** static bearing capacity of a structure. **For the Units 6 & 7 Category I structures, the computed allowable bearing capacity (including FOS = 3.0) of 39 ksf exceeds the DCD maximum static loading of 8.9 ksf.** In the case of dynamic bearing capacity, **an FOS = 2.0 is applied against** the calculated ultimate bearing capacity **in evaluating** ~~is typically compared directly against~~ the required **allowable** dynamic bearing capacity of a structure (i.e., the calculated allowable bearing capacity of subsurface materials for normal loads plus the SSE as per the DCD). ~~(~~Because the SSE in the DCD has a 0.3g peak ground acceleration that is much higher than that anticipated for South Florida, the dynamic bearing capacity in the DCD is substantially higher than the maximum dynamic loading that would be realized at the site~~)~~. For the Units 6 & 7 Category I

structures, the computed allowable bearing capacity (including FOS = 3.02.0) of 43 ksf exceeds the DCD maximum dynamic loading of 35 ksf.

The following references will be added FSAR Subsection 2.5.13 in a future revision:

2.5.4-13   References

314.   Carter, J.P. and Kulhawy, F.H., *Analysis and Design of Drilled Shaft Foundations Socketed into Rock*, Report EL-5918, Electric Power Research Institute, Palo Alto, California, 1988.

315.   Soubra, A. H., *Upper-Bound Solutions for Bearing Capacity of Foundations*, J. Geotechnical and Geoenvironmental Engineering, V. 125, No. 1, January 1999.

319.   Hoek, E, and E.T. Brown, "The Hoek-Brown Failure Criterion – a 1988 Update," Proceedings of the 15th Canadian Rock Mechanics Symposium, Toronto, 1988.

Table 2.5.4-217 will be replaced with the following in a future revision:

Table 2.5.4-217
Summary of Bearing Capacity

Evaluation Method	Foundation Width, B (ft)	Properties[1]	Local Shear Failure		Hoek-Brown[2]	Punching[3]
			Static, q_{ALL}	Dynamic, q_{ALL}	Static, q_{ALL}	Static, q_{ALL}
Rock-Only Hand Calculation	88	FD1 Rock	874	1851	67	136
Rock-Only Hand Calculation	160	FD1 Rock	1201	2320		91
Rock-Only Hand Calculation	88	FD4 Rock	597	1052	21	–
Rock-Only Hand Calculation	160	FD4 Rock	924	1500		–
Rock-Only Hand Calculation	88	LB FD4 Rock	354	706	–	–
Rock-Only Hand Calculation	160	LB FD4 Rock	583	1107	–	–
Rock & Soil Hand Calculation	88	FD4 Rock & BE Soil	129	329	–	–
Rock & Soil Hand Calculation	160	FD4 Rock & BE Soil	110	201	–	–
Rock & Soil Hand Calculation	88	LB FD4 Rock & BE Soil	93	243	–	–
Rock & Soil Hand Calculation	160	LB FD4 Rock & BE Soil	93	170	–	–
Soil-Only Hand Calculation	88	BE Soil	55	44	–	–
Soil-Only Hand Calculation	160	BE Soil	84	69	–	–
Soil-Only Hand Calculation	88	LB Soil	52	43	–	–
Soil-Only Hand Calculation	160	LB Soil	81	69	–	–
SLOPE/W	88	FD1 Rock & BE Soil	81	–	–	–
SLOPE/W	160	FD1 Rock & BE Soil	51	–	–	–
SLOPE/W	160	LB FD4 Rock & LB Soil	39	–	–	–
		Minimum:	39	43	21	91

Notes:
[1] LB Soil includes LB properties of Upper Tamiami and BE properties for Lower Tamiami and Peace River
[2] Hoek-Brown methodology is dimension independent
[3] Punching failure is based on lowest average UCS of rock layers
q_{ALL} = allowable bearing capacity
BE = Best Estimate LB = Lower Bound

The following figures will be added in a future revision

Figure 2.5.4-256
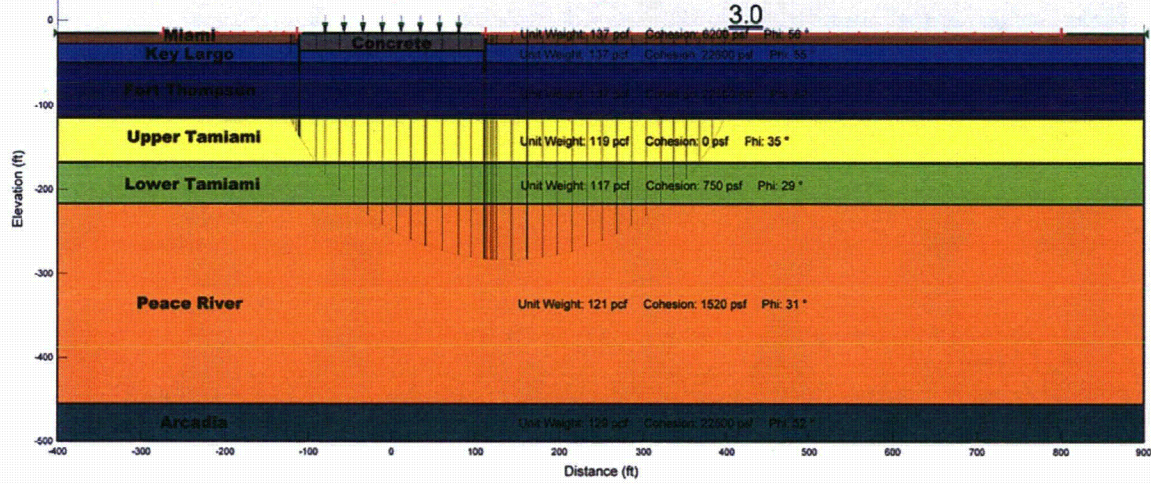**SLOPE/W Analysis of Bearing Capacity, where FS = 3.0**

Figure 2.5.4-257
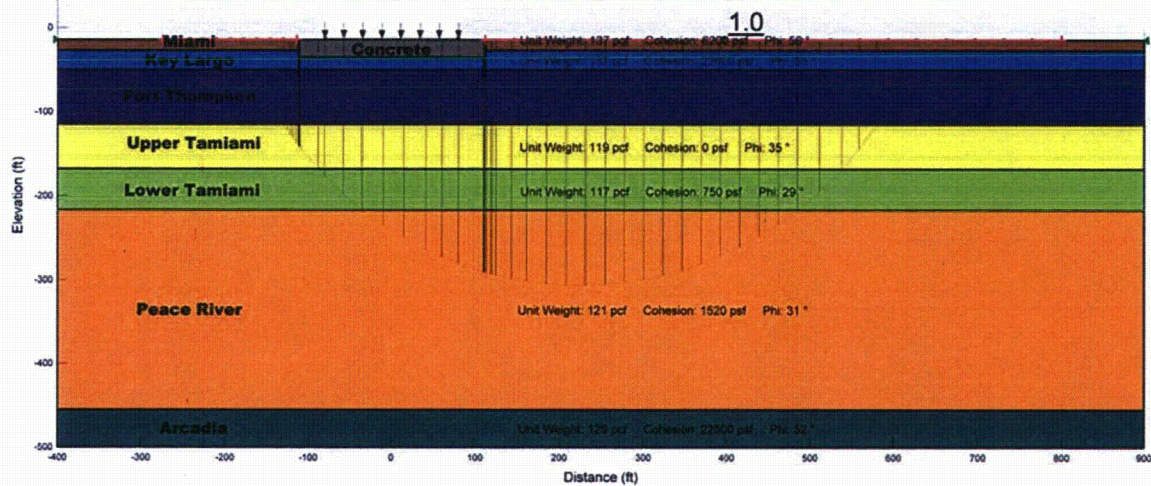**SLOPE/W Analysis of Bearing Capacity, where FS = 1.0**

Figure 2.5.4-258
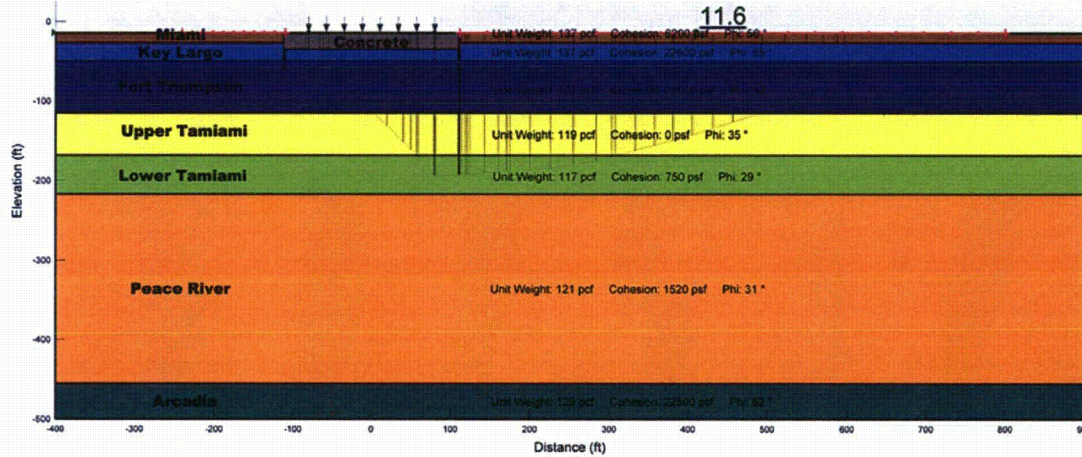**SLOPEW Analysis, 1x Required Bearing Demand**

Figure 2.5.4-259
SLOPEW Analysis with Simulated FD4 Zones, 1x Required Bearing Demand

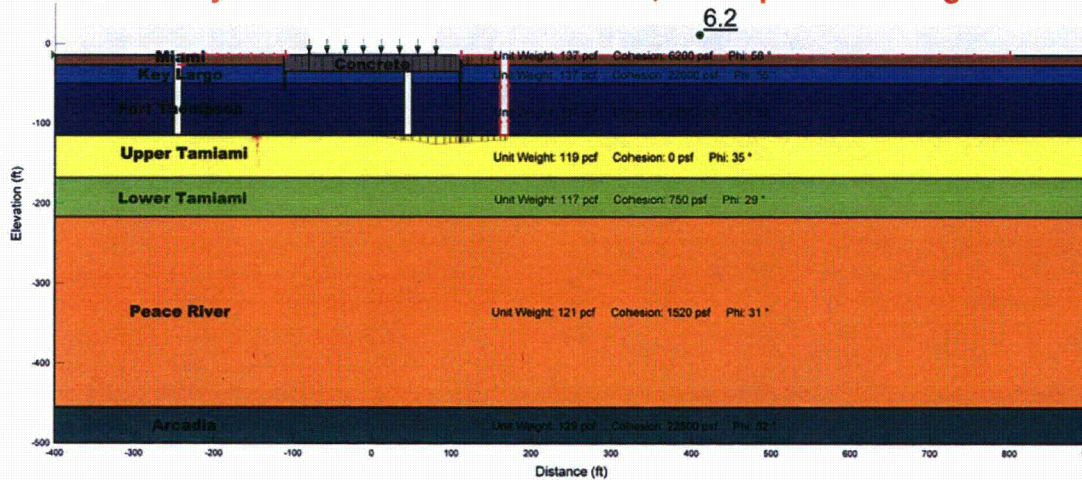**Figure 2.5.4-266**
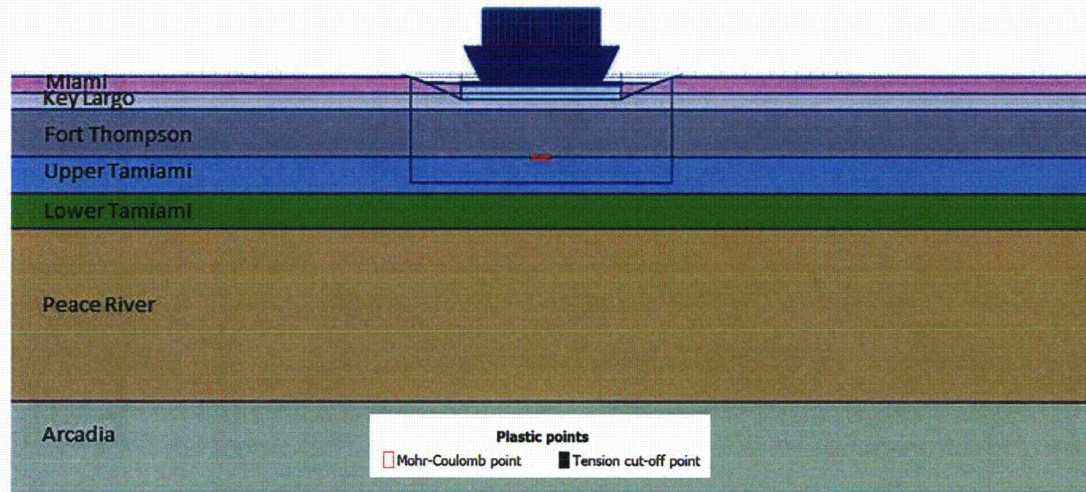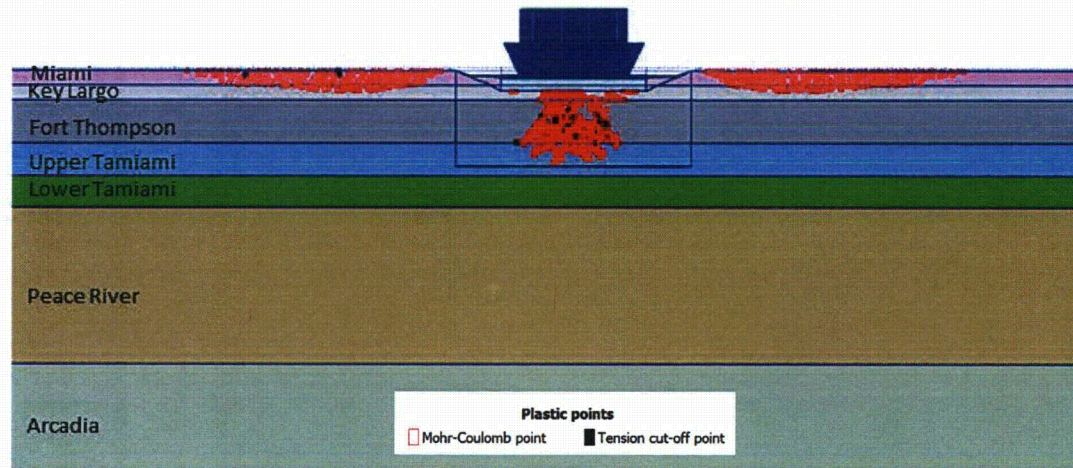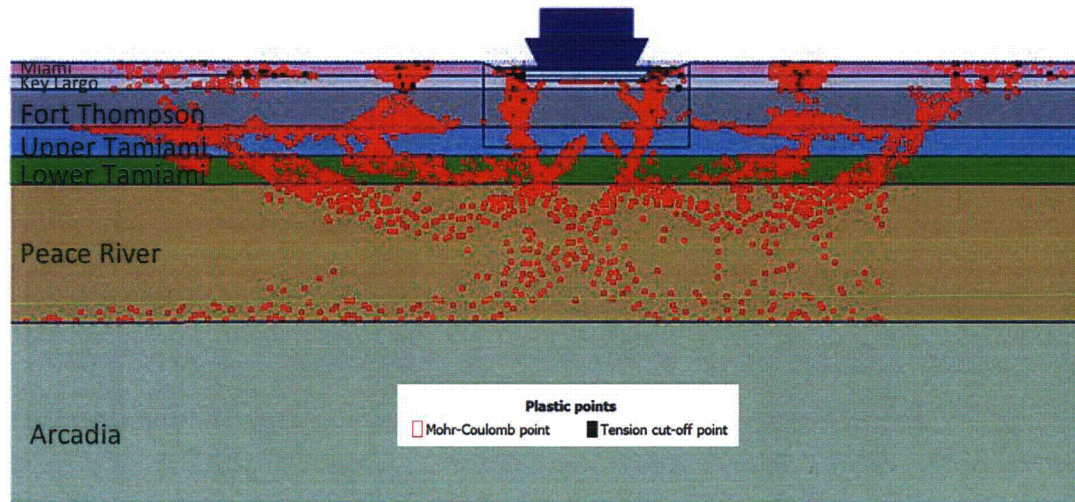**Plastic Deformation from PLAXIS 2D Analysis, 1x Required Bearing Demand**

Figure 2.5.4-267
Plastic Deformation from PLAXIS 2D Analysis, 3x Required Bearing Demand

Figure 2.5.4-268
Failure Surface from PLAXIS 2D Analysis, 60.8x Required Bearing Demand

ASSOCIATED ENCLOSURES:

None

NRC RAI Letter No. PTN-RAI-LTR-040

SRP Section: 02.05.04 - Stability of Subsurface Materials and Foundations

QUESTIONS from Geosciences and Geotechnical Engineering Branch 1 (RGS1)

NRC RAI Number: 02.05.04-19 (eRAI 6006)

AP 1000 DCD, Revision 17, Table 2.5-1 provides the total- and differential- settlement limits. The table states that the total settlement limit for the nuclear island foundation mat is 3 inches and the differential settlement limit across the nuclear island foundation mat is 0.5 inch in 50 ft. Rev.18 revised Table 2.5-1, to state that the total settlement for the nuclear island foundation mat is limited to 6 inches; however, the differential settlement limit across the nuclear island foundation mat remained 0.5 inch in 50 ft . In accordance with NUREG-0800, Standard Review Plan, Chapter 2.5.4, "Stability of Subsurface Materials and Foundations,":

    a. Please update the settlement calculations based on the DCD Rev.18 applied contact pressure for Reactor Building of 8.9 ksf instead of the 8.6 ksf stated in FSAR Rev. 2.

    b. Provide additional information describing the differential settlement calculations across the nuclear island foundation mat since values appears to exceed the acceptable limits in DCD Table 2.5-1.

    c. Provide a description of the monitoring program that will implemented to ensure that the actual settlements and differential settlements of the structures relative to the nuclear island do not exceed the DCD settlement criteria.

    d. Provide additional explanation on why and how a dynamic shear modulus degradation curve was used to compute static unidirectional settlements.

FPL RESPONSE:

The methodology for the settlement analyses of the Turkey Point Units 6 & 7 site has been revised. The settlement analyses now consist of a hand calculation that uses stress distributions appropriate for layered systems as well as a three-dimensional finite element model using PLAXIS 3D Foundation (PLAXIS 3D). Settlement analyses use the revised best estimate material properties. These updated material properties are based on laboratory data from both the initial (FSAR Section 2.5.4 Reference 257) and supplemental (FSAR Section 2.5.4 Reference 290) field investigations.

Part a:

Please update the settlement calculations based on the DCD Rev.18 applied contact pressure for Reactor Building of 8.9 ksf instead of the 8.6 ksf stated in FSAR Rev. 2.

In the revised settlement analysis, the finite element model utilizes specific foundation pressures for the shield (11.8 ksf) and auxiliary buildings (5.1 ksf for north and 7.7 ksf for south), rather than assuming one value for the entire NI. In the finite element settlement model, the areas are slightly smaller than the as-built area of the NI. The loading in the finite element model is equivalent to the average NI foundation pressure of 9.2 ksf (conservative), where the total load is equal to the uniform 8.9 ksf pressure across the NI

for as-built geometry. For consistency, the same average contact pressure of 9.2 ksf is used in the hand calculation so that the results of the two analyses are comparable.

Part b:

Provide additional information describing the differential settlement calculations across the nuclear island foundation mat since values appears to exceed the acceptable limits in DCD Table 2.5-1.

The AP1000 DCD Table 2.5-1 allows for a differential settlement across the NI foundation mat of one-half inch in 50 feet. The revised settlement hand calculation and PLAXIS 3D analyses (described in further detail below) both predict differential settlement of 0.2 inches in 50 feet. The results of the revised settlement calculations are within the acceptable limits without additional evaluation.

Part c:

Provide a description of the monitoring program that will implemented to ensure that the actual settlements and differential settlements of the structures relative to the nuclear island do not exceed the DCD settlement criteria.

A settlement monitoring program is given as one of the alternatives for the additional evaluation of settlement in DCD Section 2.5.4.3. Based on the estimated settlements of the NI, no additional evaluation is anticipated. If additional evaluation is deemed necessary, and if the settlement monitoring alternative is selected, then the program will follow the guidelines provided in the DCD regarding settlement monuments (i.e., "settlement monuments placed directly on concrete, preferably on the mudmat for early construction monitoring and on the corners of structures at grade once the mudmat monuments have been covered by backfill to be used for long-term monitoring. Monuments at grade are to be accessible with conventional surveying equipment"). The DCD also notes that there should be piezometers to measure pore pressures in a soil layer prone to consolidation type settlement. Since the soils at the Turkey Point site are not prone to consolidation type settlement, piezometers will not be used.

Part d:

Provide additional explanation on why and how a dynamic shear modulus degradation curve was used to compute static unidirectional settlements.

The dynamic shear modulus degradation curve is no longer used to compute static unidirectional settlements. A description of the revised settlement methodology and results is provided below.

Methodology of Revised Settlement Analyses:

Hand Calculation

The settlement calculation has been revised to use stress distributions appropriate for layered systems, instead of the Boussinesq distribution. For the NI, the stress distribution from Milovic (Reference 2) for a two-layered system is used. For the remaining buildings (turbine, first bay, annex, and radwaste), a stress distribution from Poulos and Davis

(Reference 3) for a three-layered system is used. The revised response to RAI 02.05.04-20 provides further information regarding the stress distributions used for the hand calculation and a comparison to the stress distributions obtained from PLAXIS 3D.

Two cases are considered in the settlement hand calculation. The first is a best estimate case using the design stiffness for each layer. The second case acts as a sensitivity analysis by using the lower bound stiffness for two layers (the upper Tamiami and Peace River). The lower bound stiffness is defined as the 16th percentile, indicating a 16 percent probability of that or a lower stiffness occurring. Therefore, the probability of having two layers with lower bound stiffness is approximately 2.5 percent. The upper Tamiami and Peace River layers are chosen for the lower bound case because they are the layers that impact settlement the most.

In the hand calculation, vertical incremental strains are calculated assuming linear elastic properties. The resulting settlement is obtained by integrating the vertical incremental strains over the soil/rock column using Equations 1 through 5 from Bowles (Reference 4).

$$\Delta\sigma_z = PI_z \hspace{4cm} \text{Equation 1}$$

Where,

σ_z = the vertical stress,
P = the building pressure,
and I_z = the percentage of building pressure at depth z

$$\Delta\sigma_h = \Delta\sigma_z * K_0 \hspace{4cm} \text{Equation 2}$$

Where,

σ_h = the horizontal stress,
and K_0 = the at rest earth pressure coefficient

$$K_0 = 1 - Sin(\varphi) \hspace{4cm} \text{Equation 3}$$

Where,

φ = the friction angle

$$\Delta\varepsilon = \frac{1}{E}\left(\Delta\sigma_z - 2v'\Delta\sigma_h\right) \hspace{3cm} \text{Equation 4}$$

Where,

$\Delta\varepsilon$ = the vertical strain,
E = the Young's modulus,
and v' = Poisson's ratio

$$\Delta S = \Delta \varepsilon * \Delta z \qquad\qquad \text{Equation 5}$$

Where,

ΔS= the settlement,
and Δz= the thickness

Heave is considered for the excavation below the NI. Dewatering will occur prior to the construction process to an elevation of -38 feet under the NI. Up to the construction of the lean concrete layer, pumping rates are assumed to create conditions of zero pressure in the bottom of the foundation (no buoyancy). Conservatively, these conditions are assumed during loading, i.e., the buoyancy forces acting to reduce settlement are neglected. The effects of buoyancy are calculated and reported separately.

Lastly, consolidation settlement is also considered using Equation 6 (Reference 4) for the lower Tamiami and Peace River layers. Consolidation settlement is found to be negligible, as expected, because the soil types at the site (upper Tamiami, lower Tamiami, and Peace River) are silty sands and are therefore not considered to be prone to consolidation type settlement. Any secondary consolidation (creep) would be even smaller than consolidation settlement, and is therefore not considered in this analysis.

$$\Delta \varepsilon = \frac{C_r}{1+e_0} * \log \frac{\sigma'_v + \Delta \sigma_z}{\sigma'_v} \qquad\qquad \text{Equation 6}$$

Where,

$\Delta \varepsilon$= the strain,
C_r = the recompression index,
e_0= the void ratio,
σ'_v= the in-situ effective stress,
and $\Delta \sigma_z$= the vertical stress

PLAXIS 3D

In addition to the settlement hand calculation, settlement is determined using PLAXIS 3D, a Finite Element Method (FEM)-based computer code designed for geotechnical analyses. The program calculates displacements with the use of numerical integration methods. In addition to the typical capabilities of a general FEM application for elastic solids, PLAXIS 3D incorporates advanced constitutive models (stress vs. strain relationship) that are capable of simulating the response of soils to external loading.

The PLAXIS 3D model includes the following phases:

1. Initial Conditions: Initial effective stresses for the soil column are obtained. The structural fill from El. -5 feet to El. 25.5 feet is already in place in this phase.

2. Dewatering: The water level, initially assumed to be at the ground surface (El. −1 feet) is lowered to El. −38 feet in the footprint of the NI. The vertical effective stresses across the depth of the soil column increase due to dewatering, causing incremental settlement.

3. Excavation and Lean Concrete Placement: Upon dewatering down to El. −38 feet, the material between El. 25.5 feet and El. −35 feet is removed in the footprint of the NI and a lean concrete backfill is installed from El. −35 feet up to El. −14 feet. In the PLAXIS 3D model, the net effect of the removal of soil/rock and the addition of the lean concrete is an incremental heave due to the drop in effective stresses across the depth. In the excavation phase, the area of the Turbine Building that is founded on El. 8.25 feet is also excavated.

4. Construction of power block structures (excluding the NI): Loads on the footprints of the turbine, first bay, radwaste, annex, and diesel generator buildings and water tanks are applied. Effective stresses increase causing incremental settlement in this stage.

5. Construction of the NI: Loads are applied on the footprint of the NI. Effective stresses increase causing incremental settlement in this stage. It is important to note that the loads on the footprint of the NI are applied while the pore pressure is assumed to be zero at the bottom of the foundation.

6. Rewatering: The water table is redefined in the PLAXIS model to be back at El. −1 foot for the NI footprint, which has the effect of generating the hydrostatic pressures acting on the bottom of the NI foundation from the stage where pumping for dewatering purposes ceased. The net effect of buoyant forces is to reduce settlements as calculated in the previous phase. However, for conservative purposes, this effect is neglected.

The actual construction sequence may involve simultaneous dewatering and excavation as well as simultaneous building construction and rewatering. The phases modeled in PLAXIS allow for determining settlements/heaves associated with each activity. Furthermore, initial conditions in the model include the backfill in place up to El. 25.5 feet. The excavation prediction, thus, includes slightly more material removal (larger heave number reported).

Nuclear Regulatory Commission RG 1.132 Appendix D states that, "Where soils are very thick, the maximum required depth for engineering purposes, denoted d_{max}, may be taken as the depth at which the change in the vertical stress during or after construction for the combined foundation loadings is less than 10% of the effective in situ overburden stress." The analysis depth of El. −450 feet, which is greater than 2B (B = the least dimension of the foundation), was assumed to be adequate to meet the aforementioned criterion. In situ initial overburden effective vertical stress at the bottom of the model is 31,303 pounds per square foot (psf). The vertical effective stress at the bottom of the model becomes: 32,299 psf at the end of excavation, 32,694 psf at the end of loading other buildings, 33,262 psf at the end of loading the NI, and 31,781 psf at the end of rewatering. The changes in effective vertical stresses are less than 10 percent of the effective in situ stress for each phase, demonstrating that the model depth is appropriate.

The plan dimensions considered in the model are 1724 feet by 1396 feet. The total displacement at the corner of the model is less than 0.1 inches, confirming that the horizontal extent of the model is appropriate.

The foundations are considered as plate elements with a thickness corresponding to the basemat thickness. The plate elements have no self weight, as the building is assumed to be inclusive of the foundation weight.

The analysis uses 15-node wedge elements. Total number of elements is 70,152 for the design mesh. The boundary conditions for the sides of the model are set to allow for the vertical displacement, and restrain the two horizontal displacement components in the x- and z- directions. The bottom of the model is restrained in the vertical and horizontal directions.

The four following sensitivity analyses are included in the PLAXIS 3D calculation:

1.   Mesh Sensitivity:

Four models with the following numbers of elements are considered: Very Coarse – 11,514, Moderately Coarse – 25,650, Design – 70,152 and Finest – 115,810. The change in mesh density for these models is focused on the loaded areas. Both vertical and horizontal meshes are varied. These models have the best estimate material properties (slightly fractured [FD1], for rock). Figure 1 shows the design mesh.

Figure 1. PLAXIS 3D Design Mesh
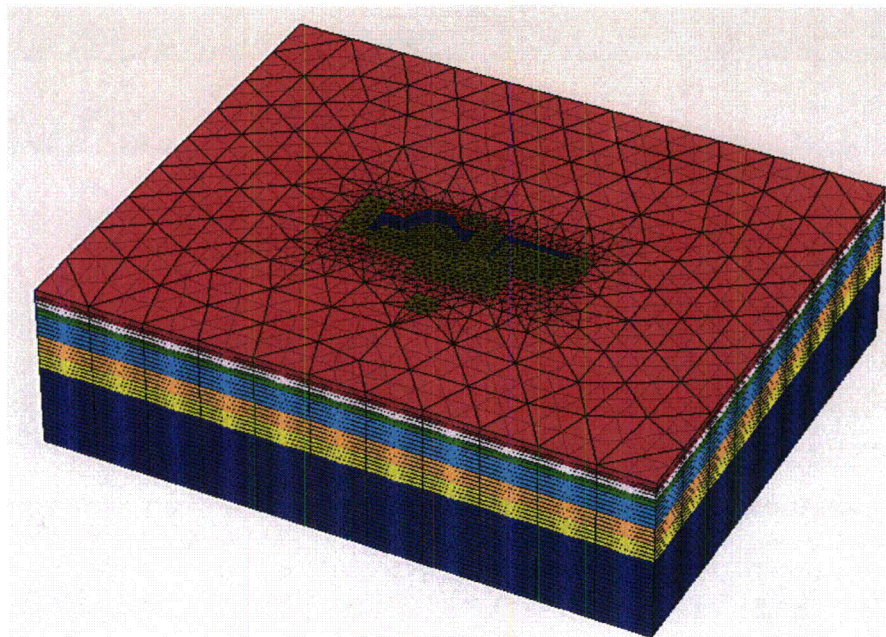
2.   Fracture Density:

Two main fracture zones are identified: slightly fractured (FD1) and moderately fractured (FD4). The zone of moderately fractured rock is significantly smaller than the zone of slightly fractured rocks as shown in Figure 2. The stiffness of the FD4 zone is less than the FD1 zone. However, the effect of including FD4 zone in the 3D settlement model is anticipated to be negligible, since the settlement is governed by the lower stiffness of the soil layers. An additional sensitivity run is conducted to check this assumption. FD4 zones are incorporated into the model, assuming FD4 zones for Unit 6, since an FD4 zone extends below the Unit 6 NI, and the fracture density is higher for Unit 6 than for Unit 7 (Figure 2). Best estimate material properties are used for soil, and FD1 properties are used for the remaining rock.

Figure 2 Estimated Location of Moderately Fractured (FD4) Zones
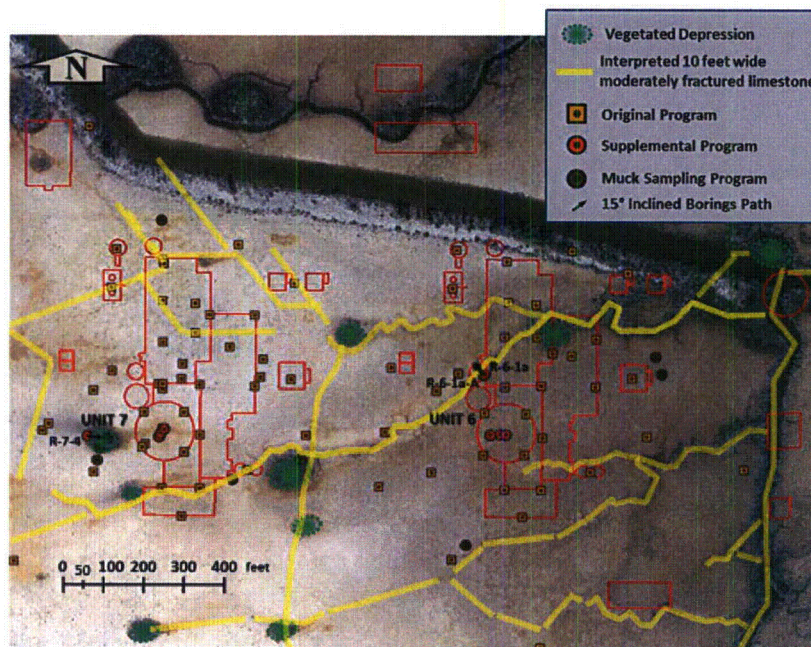
Google earth image 1/30/2005 U.S. Geological Survey

Note: Locations not marked as moderately fractured (FD4) are considered to be slightly fractured (FD1)

3.   Soil Constitutive Behavior

Soil layers are modeled using an elasto-plastic Mohr-Coulomb model, since the strain levels are expected to be low and within the relatively elastic range. The use of a Mohr-Coulomb model also dictates the use of the constant stiffness throughout soil layers. This assumption is justified based on the insensitivity that the shear wave velocity shows against depth for the soil layers, particularly for the upper and lower Tamiami formations. To check this assumption, a more comprehensive Hardening Soil model is adopted for the soil layers.

The hardening soil model is a hyperbolic model developed based on the theory of plasticity. The hardening soil model accounts for the stress-dependency of the soil stiffness by increasing stiffness with increasing pressure. When the soil experiences reloading, such as foundation loading after excavation, the hardening soil model will account for the previous stress history. This is because the reloading stiffness is typically about three to five times higher than the loading stiffness. Unlike the loading portion of the stress-strain curve, the reloading portion of the stress-strain curve is linear. The reloading stiffness is used during the reloading until the stresses induced by the applied load exceed the stresses that the soil has previously experienced; at that point, PLAXIS 3D automatically switches to using the reloading portion of the hyperbolic curve.

To determine the material properties to use in the Hardening Soil model (triaxial stiffness E_{50}, triaxial unloading stiffness E_{ur}, and the oedometer loading stiffness E_{oed}), a calibration was done varying the material parameters, while keeping the E_u/E_i ratio constant, until the stress-strain plot from PLAXIS 3D matches the stress-strain plots from the triaxial testing results. Figures 3 through 5 shows the plots of the hardening soil calibration, where all the triaxial test results from each layer are shown, along with the soil hardening based PLAXIS 3D curves at the mid-depth, top, and bottom of each layer. In addition, Figures 3 through 5 show the Mohr-Coulomb stress-strain curves obtained from PLAXIS 3D best estimate model.

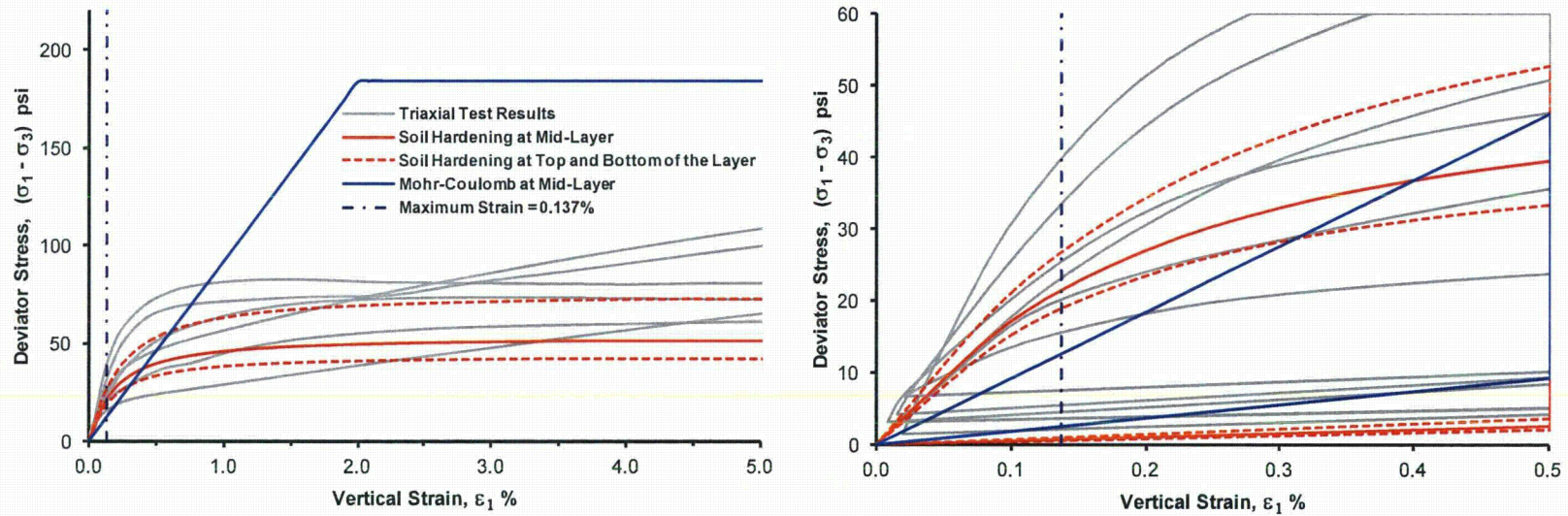Figure 3 Plot of Soil Hardening Calibration for the Upper Tamiami

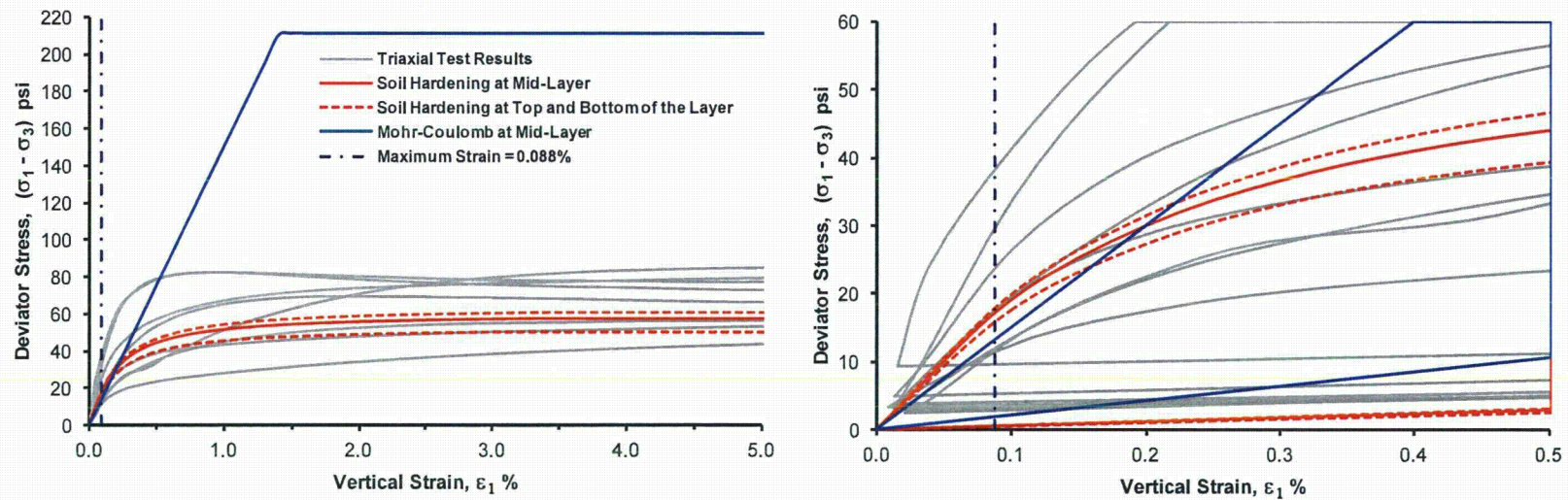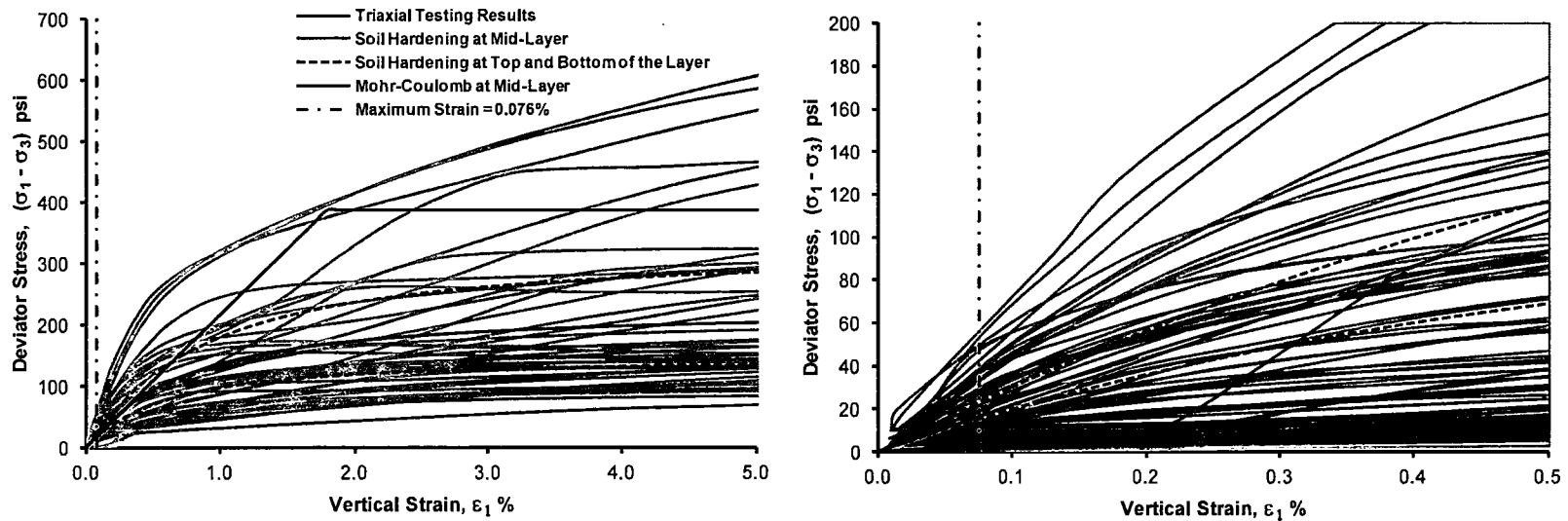## Figure 4 Plot of Soil Hardening Calibration for the Lower Tamiami

Figure 5 Plot of Soil Hardening Calibration for the Peace River

4.   Lower Bound

For the lower bound model, soil layers (upper Tamiami, lower Tamiami, and Peace River) are given lower bound stiffness values, defined as the 16th percentile, indicating a 16 percent probability of that or a lower stiffness occurring. The details of how to obtain lower bound soil parameters are provided in the revised response to RAI 02.05.04-09. The rock layers are given FD1 stiffness values.

Results of the Revised Settlement Analyses:

The following PLAXIS 3D results do not include the excavation and dewatering phases because the basemat is expected to be placed and leveled before the structural loads are applied, and excess pore pressures generated prior to basemat placement are considered to be dissipated. Therefore, monitored settlements on the basemat will not reflect the effects of dewatering and excavation. In the PLAXIS 3D model, the average heave of the NI due to excavation is estimated to be 0.5 inches.

Table 1 shows the results of the mesh sensitivity analysis. Maximum settlement predicted for the NI varies from the design mesh by 0.10 percent, 0.05 percent, and 0.14 percent for the coarse, moderately coarse, and finest meshes, respectfully. Based on these results, the design mesh is confirmed to be appropriate for the settlement analysis.

Table 1

Comparison of Mesh Sensitivity Results in the Loading Phases

Maximum Settlement (in)		Nuclear Island	Turbine Building Interior	Turbine Building Exterior	Annex Building	First Bay Building	Radwaste Building	Ancillary Water Tank	Condensate Water Tank	Diesel Generator
Load Other Buildings	Design	----	2.03	2.05	2.04	1.92	1.02	1.86	1.89	0.86
	Coarse	----	2.02	2.04	2.04	1.93	0.99	1.92	1.92	0.84
	Moderately Coarse	----	2.03	2.05	2.04	1.93	1.01	1.88	1.90	0.84
	Finest		2.04	2.05	2.04	1.92	1.02	1.84	1.88	0.86
Load NI[1]	Design	2.52	2.89	3.02	2.99	2.99	2.15	3.09	2.93	1.35
	Coarse	2.52	2.89	3.00	3.00	2.97	2.12	3.16	2.95	1.33
	Moderately Coarse	2.52	2.89	3.01	2.99	3.00	2.16	3.12	2.94	1.33
	Finest	2.52	2.90	3.01	2.98	2.98	2.15	3.07	2.92	1.35

[1]   The loading NI phase is inclusive of the previous phase.

Table 2 shows the results of the fracture density, hardening soil, and lower bound sensitivity analyses for the PLAXIS 3D models. Maximum settlement predicted for the NI varies by 1.4 percent between the model without fractures and the model with FD4 fractures. This confirms that the effect of including FD4 zone in the 3D settlement model is negligible, since the settlement is governed by the lower stiffness of the soil layers. Maximum settlement predicted for the NI varies by 1.6 percent based on the type of model (Mohr-Coulomb or hardening soil), confirming that the Mohr-Coulomb best estimate model is appropriate. The maximum settlement predicted for the NI varies by 29.9 percent between the lower bound and best estimate cases, again confirming that the settlement is governed by the lower stiffness of the soil layers.

Table 2
Fracture Density, Hardening Soil, and Lower Bound Sensitivity Analyses

Maximum Settlement (in)		Nuclear Island	Turbine Building Interior	Turbine Building Exterior	Annex Building	First Bay Building	Radwaste Building	Ancillary Water Tank	Condensate Water Tank	Diesel Generator
Load Other Buildings	Best Estimate	----	2.0	2.0	2.0	1.9	1.0	1.9	1.9	0.9
	Lower Bound	----	2.5	2.5	2.5	2.4	1.3	2.3	2.3	1.2
	Soil Hardening	----	1.9	1.9	1.9	1.8	0.9	1.7	1.7	0.8
	Fractured Zone	----	2.1	2.1	2.1	2.0	1.0	1.9	1.9	0.9
Load NI[1]	Best Estimate	2.5	2.9	3.0	3.0	3.0	2.1	3.1	2.9	1.3
	Lower Bound	3.4	3.7	3.9	3.8	3.9	2.9	3.9	3.8	2.0
	Soil Hardening	2.5	3.0	3.1	3.0	3.0	2.1	3.1	3.0	1.5
	Fractured Zone	2.6	3.0	3.1	3.0	3.0	2.2	3.1	3.0	1.4
Rewatering	Best Estimate	2.1	2.6	2.7	2.7	2.7	1.8	2.7	2.6	1.1
	Lower Bound	2.9	3.3	3.4	3.4	3.4	2.4	3.4	3.3	1.6
	Soil Hardening	2.3	2.8	2.9	2.9	2.9	2.0	2.9	2.8	1.4
	Fractured Zone	2.2	2.6	2.7	2.7	2.7	1.8	2.8	2.6	1.1

[1]   The loading NI phase is inclusive of the previous phase.

The sensitivity analyses presented in Tables 1 and 2 demonstrate that the best estimate model used is appropriate. Figure 6 shows the PLAXIS 3D total displacement output for the best estimate model after the loading of the NI. Figure 7 shows the PLAXIS 3D total displacement output for the best estimate model after rewatering.

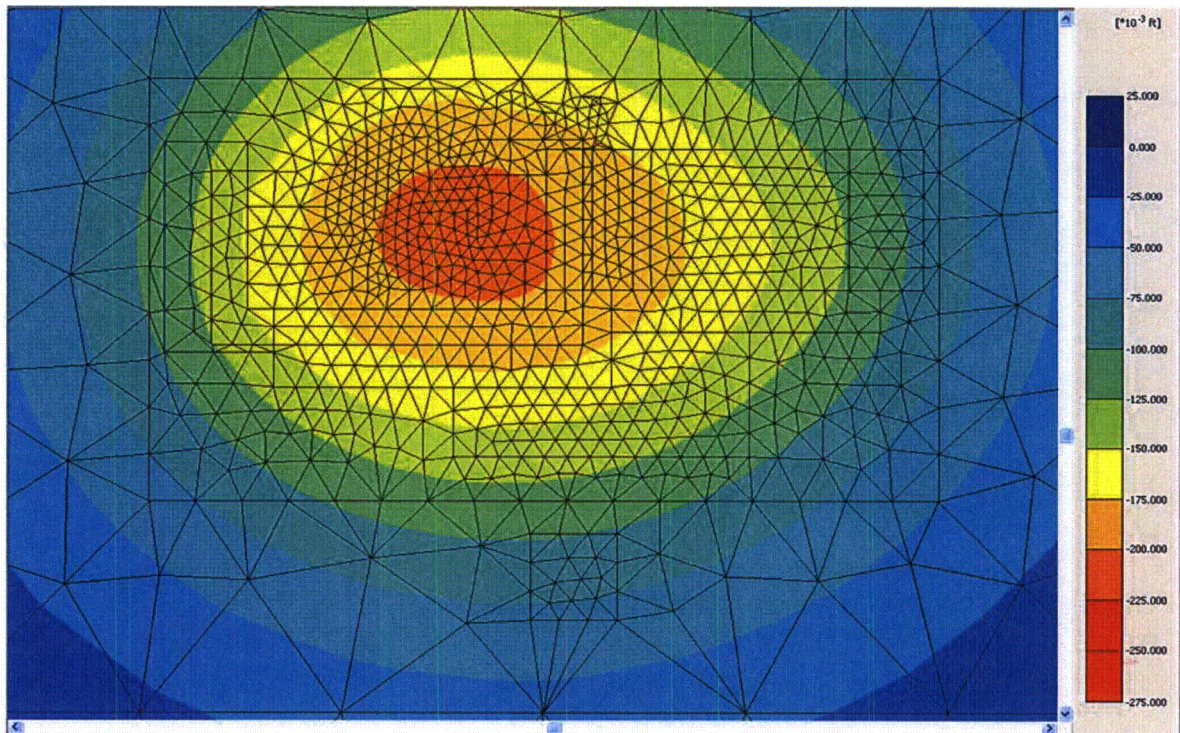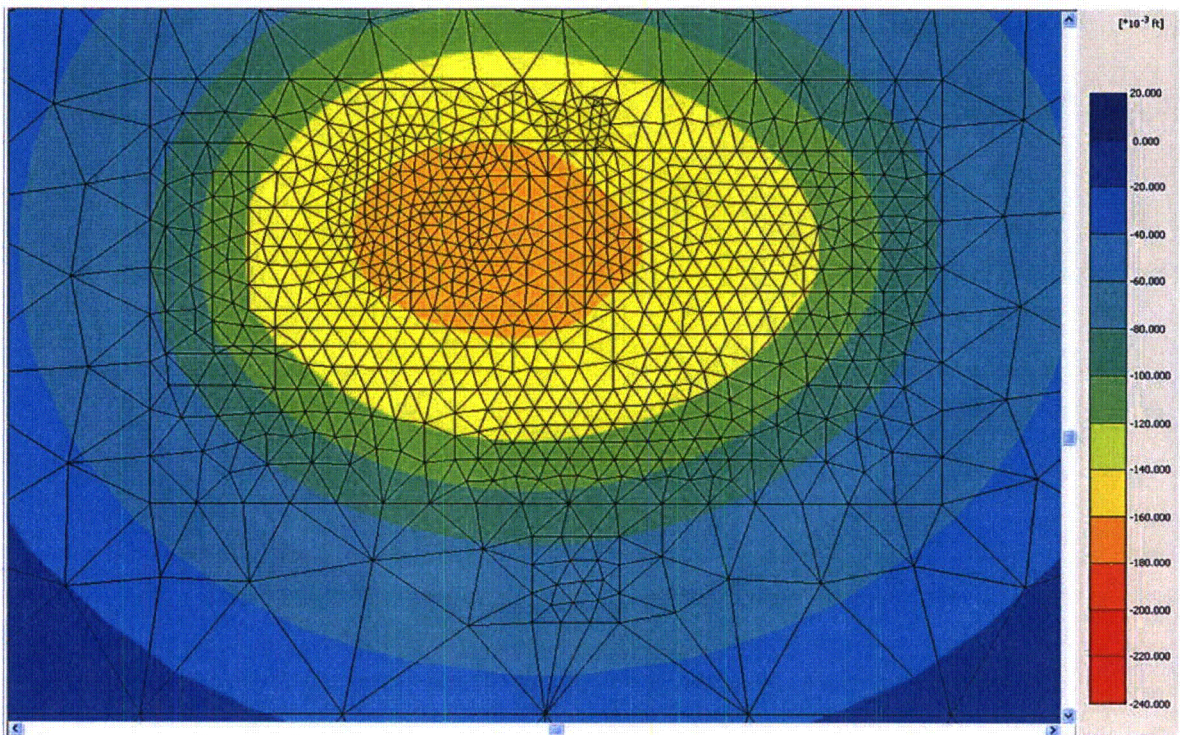**Figure 6 PLAXIS 3D Best Estimate Model Total Settlement After Loading**

Figure 7 PLAXIS 3D Best Estimate Model Total Settlement After Rewatering

Table 3 shows the comparison between the settlement predicted by the hand calculation and PLAXIS 3D model to the DCD requirements. The lower bound and best estimate cases for the hand calculation and the PLAXIS 3D model are within the acceptable limits provided by the DCD.

Table 3

Comparison of Limits of Acceptable Settlement without Additional Evaluation

		Differential Across Nuclear Island Foundation Mat (in per 50 ft)	Total for Nuclear Island Foundation Mat (in)	Differential Between Nuclear Island and Turbine Building[1] (in)	Differential Between Nuclear Island and Other Buildings[1][2] (in)
DCD Requirement		0.5	6	3	3
Best Estimate	Plaxis 3D	0.20	2.5	0.5	1.6
	Hand Calculation	0.21	2.3	0.5	1.9
Lower Bound	Plaxis 3D	0.23	3.4	0.9	2.2
	Hand Calculation	0.25	3.1	0.8	2.6

[1] Differential settlement is measured at the center of the nuclear island and the center of adjacent structures.

[2] Maximum differential settlement occurs between NI and radwaste buildings.

[3] Settlements presented exclude the rewatering phase

The revised settlement analyses, including the hand calculation and PLAXIS 3D model, show that the predicted best estimate settlement is within the limits provided by the DCD.

This response is PLANT SPECIFIC.

References:

1. Westinghouse Electric Company, AP1000 Design Control Document (DCD), Revision 19, June 21, 2011.

2. Milovic, D., Stresses and Displacements for Shallow Foundations, Elsevier, 1992.

3. Poulos, H. G. and E.H. Davis, Elastic Solutions for Soil and Rock Mechanics, John Wiley & Sons, Inc., 1974.

4. Bowles, J. E., Foundation Analysis and Design, Fifth Edition, McGraw-Hill, Inc., 1997.

ASSOCIATED COLA REVISIONS:

FSAR Subsection 2.5.4.10.3 will be revised in a future revision as follows:

The settlement analyses consist of a hand calculation that uses stress distributions appropriate for layered systems as well as a three-dimensional finite element model using PLAXIS 3D Foundation (PLAXIS 3D). Settlement analyses use the revised best estimate material properties. These updated material properties are based on laboratory data from both the initial (Reference 257) and supplemental (Reference 290) field investigations.

~~Foundation settlements are estimated using pseudo-elastic compression methods. Based on a stress-strain model that computes settlement in discrete layers, the settlement of shallow foundations due to elastic compression of subsurface materials is estimated as:~~

~~$\delta = \Sigma (\Delta p_i h_i)/E_i$~~   ~~Equation 2.5.4-21~~

~~Where,~~

> ~~δ = settlement~~
> ~~i = 1 to n, where n is the number of layers~~
> ~~Δp_i = vertical applied pressure at the center of layer i~~
> ~~h_i = thickness of layer i~~
> ~~E_i = elastic modulus of layer i~~

~~The stress distribution below the corner of a rectangular flexible foundation is based on a Boussinesq type distribution (Reference 225):~~

~~$\sigma_z = (p/2\pi) \{\tan^{-1}[l\,b/(z\,R3)] + (l\,b\,z/R3)(1/R1^2 + 1/R2^2)\}$~~   ~~Equation 2.5.4-22~~

~~Where,~~

> ~~l = length of the footing~~
> ~~b = width of footing~~
> ~~z = depth below footing at which pressure is computed~~
> ~~$R1 = (l^2 + z^2)^{0.5}$~~
> ~~$R2 = (b^2 + z^2)^{0.5}$~~
> ~~$R3 = (l^2 + b^2 + z^2)^{0.5}$~~

~~Note that to calculate σ_z values below the midpoint of an edge and below the center of a rectangular foundation, the values of σ_z calculated from Equation 2.5.4-22 above are multiplied by two and four, respectively, to obtain p_i, the vertical applied pressure at the center of layer i for use in Equation 2.5.4-21.~~

The containment and auxiliary buildings (nuclear island) share the same mat foundation and are founded on lean concrete placed above rock of the Key Largo Limestone. Therefore, for settlement computations, the bottom of the foundation is taken at El. −14 feet on lean concrete. **The best estimate** ~~S~~settlement of the rock **and soil** strata is computed using the elastic modulus values tabulated in Table 2.5.4-209. ~~Settlement of the soil strata is evaluated using the strain compatible elastic moduli of the Tamiami and Peace River Formations with corresponding axial strains, as discussed later in this section.~~ The elastic modulus for the lean concrete used for settlement estimates is derived as follows:

The thickest part of lean concrete is between El. −14 feet and El. −35 feet, i.e., 21 feet thick (see Figure 2.5.4-222). The elastic modulus of lean concrete with a unit weight of **150**~~145~~ pcf can be calculated using the following equation (Reference ~~274~~**317**).

~~$E_c = 1820 \cdot f'_c{}^{0.5}$ (ksi)~~   ~~Equation 2.5.4-23~~

$$E_c = 57,000\sqrt{f'_c} \text{ (psi)} \qquad\qquad \textbf{Equation 2.5.4-21}$$

where,

f'c = specified compressive strength of concrete (~~ksi~~**psi**)

The lean concrete placed on rock is expected to have a minimum compressive strength of ~~1.5 ksi.~~**1500 psi.**

~~f'c = 1.5 ksi, then Ec = 1820·1.50.5 = 2229 ksi ≈ 321,000 ksf~~

$$f'_c = 1.5\ ksi, then\ E_c = 57,000\sqrt{1500} = 2.21 * 10^6 psi \approx 318,500\ ksf$$

~~The settlements under the nuclear island foundation with plan dimensions of 88 feet by 254 feet and 159 feet by 254 feet are calculated with an applied pressure of 8.9 ksf. The estimated total settlements at the center and at midpoints of the sides are largely impacted by the large foundation size and loading, and by the elastic modulus values of the soil strata. The preconsolidated soils of the Tamiami and Peace River Formations are confined below an 80-foot-thick stratum of rock, and thus a relatively low settlement estimate is expected from these dense granular and stiff fine-grained layers. Settlements at the center of the mat foundations are evaluated using the strain-compatible elastic moduli of the Tamiami and Peace River Formations with corresponding axial strains. The strain compatible evaluation is performed only for the soil strata, i.e., the Tamiami and Peace River Formations where there is a difference between the high and low strain moduli. In order to apply the elastic moduli in Equation 2.5.4-21, their values need to be equated with strain level. In this case, the modulus degradation with increasing strain is based on the recommended curves in Figure 2.5.4-233 after converting shear strain to axial strain.~~

~~For calculating settlement of structures using the elastic method, the maximum principal strain is the vertical strain (i.e., $\varepsilon_1 = \varepsilon_v$), while the minimum principal strain is assumed to be zero (i.e., $\varepsilon_3 = 0$). Because the maximum shear strain $\gamma_{max} = \varepsilon_1 - \varepsilon_3 = \varepsilon_1$ (Reference 275) and $E/E_{max} = G/G_{max}$, the elastic modulus reduction curves with respect to vertical strain should be the same as the shear modulus reduction curves with respect to the shear strain. Therefore, the strain levels in degradation curves (Figure 2.5.4-233) are interchangeable between the shear strain and axial strain without any need of correction. Thus, the same degradation curve in Figure 2.5.4-233 with G/G_{max} on the vertical axis and percent shear strain on the horizontal axis can be used to determine appropriate values of E for settlement calculations. The ratio of E/E_{max} is equivalent to G/G_{max} and the computed percent axial strain corresponds to the percent shear strain using Figure 2.5.4-233.~~

~~A trial process is followed for soil Strata 5, 6, and 7 using the degradation curves to arrive at a compatible axial strain, such that the strain for the adopted modulus and the calculated strain converge. For rock and concrete strata, the settlements computed are based on a constant (not strain dependent) elastic modulus. The results of the settlement analysis on Table 2.5.4-219 show the computed settlements at the center and edge of the nuclear island foundations with dimensions of 88 feet by 254 feet and 159 feet by 254 feet, under loading of 8.9 ksf. (Two sets of plan dimensions are used because of the irregular shape of the foundation.) Similar settlement calculations are made for the turbine, annex and radwaste buildings, and the results are presented in Table 2.5.4-219. As with the nuclear~~

island, settlements of the annex building are analyzed for two sets of foundation
dimensions.

As noted earlier, Equation 2.5.4-22 computes the stress distribution beneath a flexible
foundation, which accounts for the sometimes significant difference in computed settlement
between the center of the foundation and the mid-point of the side of the foundation. In fact,
the foundations of the structures listed in Table 2.5.4-219 are thick, reinforced concrete
mats with appreciable structural stiffness. Thus the mean settlements listed in Table 2.5.4-
219 more closely reflect the actual anticipated settlements across the whole foundation.
Table 2.0-201 lists the DCD limits of acceptable settlement without need for additional
evaluation. Limits for the nuclear island are 6 inches total settlement and a differential
settlement across the nuclear island foundation mat of one-half inch in 50 feet. The Table
2.5.4-219 values are within the limits for total settlement. The values for differential
settlement are within the limits for Case I and outside the limits for Case II. However, as
noted above, the Table 2.5.4-219 values assume a flexible foundation, and the actual
differential settlement across the thick, reinforced mat foundation is negligible. Table 2.0-
201 also lists limits of differential settlement between the nuclear island and surrounding
structures as 3 inches. The difference between the estimated settlement of the nuclear
island and the settlement of the surrounding structures in Table 2.5.4-219, i.e., the
differential settlement, is within the limits. As noted below, because of the nature of the
soils and rock underlying the new units, post-construction settlement will be negligible.

Because the construction of each unit is over a period of greater than five years, the elastic
settlement estimated in Table 2.5.4-219 is essentially complete prior to the start of
operation of the unit. No time-dependent consolidation settlement is anticipated. Any
additional settlement after completion is considered not significant.

FSAR Subsection 2.5.4.10.3.1 will be added in a future revision as follows:

2.5.4.10.3.1 Hand Calculation of Settlement

In the hand calculation, vertical incremental strains are calculated assuming linear
elastic properties. The resulting settlement is obtained by integrating the vertical
incremental strains over the soil/rock column using Equations 2.5.4-22a through
2.5.4-22e (Reference 217).

Two cases are considered in the settlement hand calculation. The first is a best
estimate case using the design stiffness for each layer. The second case acts as a
sensitivity analysis by using the lower bound stiffness for two layers (the upper
Tamiami and Peace River). The lower bound stiffness is defined as the 16th
percentile, indicating a 16 percent probability of that or a lower stiffness occurring.
Therefore, the probability of having two layers with lower bound stiffness is
approximately 2.5 percent. The upper Tamiami and Peace River layers are chosen for
the lower bound case because they are the layers that impact settlement the most.
Average lower bound properties are given in Table 2.5.4-221.

The Key Largo Limestone and the Fort Thompson Formation form a stiff upper layer,
while the layers below (upper Tamiami, lower Tamiami, and Peace River) are
comprised primarily of dense, silty sands. Because of this layering, a typical

Boussinesq stress distribution may not provide realistic stress distributions, showing very high settlement in the deep sand layers. Therefore, stress distributions appropriate for layered systems are used.

For the NI, a stress distribution from Milovic (Reference 316) for a two-layered system was used with rock (Key Largo and Fort Thompson) as the first layer and soil (upper Tamiami, lower Tamiami, and Peace River) as the second layer. For the remaining buildings (turbine, first bay, annex, and radwaste), a stress distribution from Poulos and Davis (Reference 275) for a three-layered system was used with the fill as the first layer; rock (Miami Limestone, Key Largo, and Fort Thompson) as the second layer; and soil (upper Tamiami, lower Tamiami, and Peace River) as the third layer. In each case, the stress distribution is dependent on the stiffness and thickness of each layer, the area of the building, and the depth of interest. The stress distributions assume a circular foundation. Based on the layering information, Iz coefficients, defined as the percentage of the building pressure, are found.

$$\Delta\sigma_z = PI_z \qquad\qquad \text{Equation 2.5.4-22a}$$

Where,

σ_z = the vertical stress,
P = the building pressure,
and I_z = the percentage of building pressure at depth z

$$\Delta\sigma_h = \Delta\sigma_z * K_0 \qquad\qquad \text{Equation 2.5.4-22b}$$

Where,

σ_h = the horizontal stress,
and K_0 = the at rest earth pressure coefficient

$$K_0 = 1 - Sin(\varphi) \qquad\qquad \text{Equation 2.5.4-22c}$$

Where,

φ = the friction angle

$$\Delta\varepsilon = \frac{1}{E}\left(\Delta\sigma_z - 2v'\Delta\sigma_h\right) \qquad\qquad \text{Equation 2.5.4-22d}$$

Where,

$\Delta\varepsilon$ = the vertical strain,
E = the Young's modulus,
and v' = Poisson's ratio

$$\Delta S = \Delta\varepsilon * \Delta z \qquad\qquad \text{Equation 2.5.4-22e}$$

Where,

> ΔS= the settlement,
> and Δz= the thickness

Heave is considered for the excavation below the NI. Dewatering will occur prior to the construction process to an elevation of -38 feet under the NI. Up to the construction of the lean concrete layer, pumping rates are assumed to create conditions of zero pressure in the bottom of the foundation (no buoyancy). Conservatively, these conditions are assumed during loading, i.e., the buoyancy forces acting to reduce settlement are neglected. The effects of buoyancy are calculated and reported separately.

Lastly, consolidation settlement is also considered using Equation 2.5.4-23 (Reference 217) for the lower Tamiami and Peace River layers. Consolidation settlement is found to be negligible, as expected, because the soil types at the site (upper Tamiami, lower Tamiami, and Peace River) are silty sands and are therefore not considered to be prone to consolidation type settlement. Any secondary consolidation (creep) would be even smaller than consolidation settlement, and is therefore not considered in this analysis.

$$\Delta\varepsilon = \frac{C_r}{1+e_0} * \log\frac{\sigma'_v+\Delta\sigma_z}{\sigma'_v} \qquad\qquad \text{Equation 2.5.4-23}$$

Where,

> $\Delta\varepsilon$= the strain,
> C_r = the recompression index,
> e_0= the void ratio,
> σ'_v= the in-situ effective stress,
> and $\Delta\sigma_z$= the vertical stress

FSAR Subsection 2.5.4.10.3.2 will be added in a future revision as follows:

2.5.4.10.3.2   PLAXIS 3D Settlement Model

In addition to the settlement hand calculation, settlement is determined using PLAXIS 3D, a Finite Element Method (FEM)-based computer code designed for geotechnical analyses. The program calculates displacements with the use of numerical integration methods. In addition to the typical capabilities of a general FEM application for elastic solids, PLAXIS 3D incorporates advanced constitutive models, (stress vs. strain relationship) that are capable of simulating the response of soils to external loading.

The PLAXIS 3D model includes the following phases:

1. Initial conditions: Initial effective stresses for the soil column are obtained. The structural fill from El. −5 feet to El. 25.5 feet is already in place in this phase.

2. Dewatering: The water level, initially assumed to be at the ground surface (El. −1 feet) is lowered to El. −38 feet in the footprint of the NI. The vertical effective stresses across the depth of the soil column increase due to dewatering, causing incremental settlement.

3. Excavation and lean concrete placement: Upon dewatering down to El. −38 feet, the material between El. 25.5 feet and El. −35 feet is removed in the footprint of the NI and a lean concrete backfill is installed from El. −35 feet up to El. −14 feet. In the PLAXIS 3D model, the net effect of the removal of soil/rock and the addition of the lean concrete is an incremental heave due to the drop in effective stresses across the depth. In the excavation phase, the area of the Turbine Building that is founded on El. 8.25 feet is also excavated.

4. Construction of power block structures (excluding the NI): Loads on the footprints of the turbine, first bay, radwaste, annex, and diesel generator buildings and water tanks are applied. Effective stresses increase causing incremental settlement in this stage.

5. Construction of the NI: Loads are applied on the footprint of the NI. Effective stresses increase causing incremental settlement in this stage. It is important to note that the loads on the footprint of the NI are applied while the pore pressure is assumed to be zero at the bottom of the foundation.

6. Rewatering: The water table is redefined in the PLAXIS model to be back at El. −1 for the NI footprint, which has the effect of generating the hydrostatic pressures acting on the bottom of the NI foundation from the stage where pumping for dewatering purposes ceased. The net effect of buoyant forces is to reduce settlements as calculated in the previous phase. However, for conservative purposes, this effect is neglected.

The actual construction sequence may involve simultaneous dewatering and excavation as well as simultaneous building construction and rewatering. The phases modeled in PLAXIS allow for determining settlements/heaves associated with each activity. Furthermore, initial conditions in the model include the backfill in place up to El. 25.5 feet. The excavation prediction, thus, includes slightly more material removal (larger heave number reported).

Nuclear Regulatory Commission RG 1.132 Appendix D states that, "Where soils are very thick, the maximum required depth for engineering purposes, denoted d_{max}, may be taken as the depth at which the change in the vertical stress during or after construction for the combined foundation loadings is less than 10% of the effective in situ overburden stress." The analysis depth of El.−450 feet, which is greater than 2B (B = the least dimension of the foundation), was assumed to be adequate to meet the aforementioned criterion. In situ initial overburden effective vertical stress at the

bottom of the model is 31,303 pounds per square foot (psf). The vertical effective stress at the bottom of the model becomes: 32,299 psf at the end of excavation, 32,694 psf at the end of loading other buildings, 33,262 psf at the end of loading the NI, and 31,781 psf at the end of the rewatering phase. The changes in effective vertical stresses are less than 10 percent of the effective in situ stress for each phase, demonstrating that the model depth is appropriate.

The plan dimensions considered in the model are 1724 feet by 1396 feet. The total displacement at the corner of the model is less than 0.1 inches, confirming that the horizontal extent of the model is appropriate.

The foundations are considered as plate elements with a thickness corresponding to the basemat thickness. The plate elements have no self weight, as the building is assumed to be inclusive of the foundation weight.

The analysis uses 15-node wedge elements. Total number of elements is 70,152 for the design mesh. The boundary conditions for the sides of the model are set to allow for the vertical displacement, and restrain the two horizontal displacement components in the x- and z- directions. The bottom of the model is restrained in the vertical and horizontal directions.

The four following sensitivity analyses are included in the PLAXIS 3D calculation:

1. Mesh Sensitivity:

    Four models with the following numbers of elements are considered: very coarse – 11,514, moderately coarse – 25,650, design – 70,152, and finest – 115,810. The change in mesh density for these models is focused on the loaded areas. Both vertical and horizontal meshes are varied. These models have the best estimate material properties (slightly fractured [FD1], for rock). Figure 2.5.4-260 shows the design mesh.

2. Fracture Density:

    Two main fracture zones are identified: slightly fractured (FD1) and moderately fractured (FD4). The zone of moderately fractured rock is significantly smaller than the zone of slightly fractured rocks as shown in Figure 2.5.4-254. The stiffness of the FD4 zone is less than the FD1 zone. However, the effect of including FD4 zone in the 3D settlement model is anticipated to be negligible, since the settlement is governed by the lower stiffness of the soil layers. An additional sensitivity run is conducted to check this assumption. FD4 zones are incorporated into the model, assuming FD4 zones for Unit 6, since an FD4 zone extends below the Unit 6 NI, and the fracture density is higher for Unit 6 than for Unit 7 (Figure 2.5.4-254). Best estimate material properties are used for soil, and FD1 properties are used for the remaining rock.

3. **Soil Constitutive Behavior:**

    Soil layers are modeled using an elasto-plastic Mohr-Coulomb model, since the strain levels are expected to be low and within the relatively elastic range. The use of a Mohr-Coulomb model also dictates the use of the constant stiffness throughout soil layers. This assumption is justified based on the insensitivity that the shear wave velocity shows against depth for the soil layers, particularly for the upper and lower Tamiami Formations. To check this assumption, a more comprehensive Hardening Soil model is adopted for the soil layers.

    The hardening soil model is a hyperbolic model developed based on the theory of plasticity. The hardening soil model accounts for the stress-dependency of the soil stiffness by increasing stiffness with increasing pressure. When the soil experiences reloading, such as foundation loading after excavation, the hardening soil model will account for the previous stress history. This is because the reloading stiffness is typically about three to five times higher than the loading stiffness. Unlike the loading portion of the stress-strain curve, the reloading portion of the stress-strain curve is linear. The reloading stiffness is used during the reloading until the stresses induced by the applied load exceed the stresses that the soil has previously experienced; at that point, PLAXIS 3D automatically switches to using the reloading portion of the hyperbolic curve.

    To determine the material properties to use in the hardening soil model (triaxial stiffness E_{50}, triaxial unloading stiffness E_{ur}, and the oedometer loading stiffness E_{oed}), a calibration was done varying the material parameters, while keeping the E_u/E_i ratio constant, until the stress-strain plot from PLAXIS 3D matches the stress-strain plots from the triaxial testing results. Figures 2.5.4-261 through 2.5.4-263 show the plots of the hardening soil calibration, where all the triaxial test results from each layer are shown, along with the soil hardening based PLAXIS 3D curves at the mid-depth, top, and bottom of each layer. In addition, Figures 2.5.4-261 through 2.5.4-263 show the Mohr-Coulomb stress-strain curves obtained from the PLAXIS 3D best estimate model.

4. **Lower Bound:**

    For the lower bound model, soil layers (upper Tamiami, lower Tamiami, and Peace River) are given lower bound stiffness values, defined as the 16th percentile, indicating a 16 percent probability of that or a lower stiffness occurring. The rock layers are given FD1 stiffness values.

FSAR Subsection 2.5.4.10.3.3 will be added in a future revision as follows:

2.5.4.10.3.3   Settlement Results

Table 2.5.4-219 shows the maximum settlement per building predicted by the hand calculation.

The following PLAXIS 3D results do not include the excavation and dewatering phases because the basemat is expected to be placed and leveled before the structural loads are applied, and excess pore pressures generated prior to basemat placement are considered to be dissipated. Therefore, monitored settlements on the basemat will not reflect the effects of dewatering and excavation. In the PLAXIS 3D model, the average heave of the NI due to excavation is estimated to be 0.5 inches.

Table 2.5.4-222 shows the results of the mesh sensitivity analysis. Maximum settlement predicted for the NI varies from the design mesh by 0.10 percent, 0.05 percent, and 0.14 percent for the coarse, moderately coarse, and finest meshes, respectfully. Based on these results, the design mesh is confirmed to be appropriate for the settlement analysis.

Table 2.5.4-223 shows the results of the fracture density, hardening soil, and lower bound sensitivity analyses for the PLAXIS 3D models. Maximum settlement predicted for the NI varies by 1.4 percent between the model without fractures and the model with FD4 fractures. This confirms that the effect of including FD4 zone in the 3D settlement model is negligible, since the settlement is governed by the lower stiffness of the soil layers. Maximum settlement predicted for the NI varies by 1.6 percent based on the type of model (Mohr-Coulomb or hardening soil), confirming that the Mohr-Coulomb best estimate model is appropriate. The maximum settlement predicted for the NI varies by 29.9 percent between the lower bound and best estimate cases, again confirming that the settlement is governed by the lower stiffness of the soil layers.

Table 2.5.4-224 shows the comparison between the settlement predicted by the hand calculation and the PLAXIS 3D model to the DCD requirements. The lower bound and best estimate cases for the hand calculation and the PLAXIS 3D model are within the acceptable limits provided by the DCD.

The sensitivity analyses presented in Tables 2.5.4-222 and 2.5.4-223 demonstrates that the best estimate model used is appropriate. Figure 2.5.4-264 shows the PLAXIS 3D total displacement output for the best estimate model after the loading of the NI. Figure 2.5.4-265 shows the PLAXIS 3D total displacement output for the best estimate model after rewatering.

FSAR Subsection 2.5.13 in will be revised in a future revision as follows:

274. American Association of State Highway and Transportation Officials, *LRFD Bridge Design Specification*, 2d ed., Washington, D.C., 1998.

316. Milovic, D., *Stresses and Displacements for Shallow Foundations*, Elsevier, 1992.

317. American Concrete Institute, *Building Code Requirements for Structural Concrete and Commentary*, ACI 318-11, 2011.

FSAR Table 2.5.4-219 will be replaced with the following revised table in a future revision:

Table 2.5.4-219
Estimated Foundation Settlements

Structure	Contact Pressure (ksf)	Subsurface	Area (ft^2)	Hand Calculation Best Estimate Maximum Settlement[2] (inch)
Reactor & Auxiliary	9.2	Lean Concrete Fill on Rock	31,318	2.3
Turbine	4.2	Compacted Fill	41,925	1.8
First Bay	3.7	Compacted Fill	4,740	0.9
Annex[1]	2.4	Compacted Fill	19,888	0.9
Radwaste	1.3	Compacted Fill	13,363	0.4

[1] Excludes annex office building.
[2] Excludes heave due to rewatering.

The following Tables will be added in a future revision:

Table 2.5.4-222

Comparison of Mesh Sensitivity Results in the Loading Phases

Maximum Settlement (inch)		Nuclear Island	Turbine Building Interior	Turbine Building Exterior	Annex Building	First Bay Building	Radwaste Building	Ancillary Water Tank	Condensate Water Tank	Diesel Generator
Load Other Buildings	Design	–	2.03	2.05	2.04	1.92	1.02	1.86	1.89	0.86
	Coarse	–	2.02	2.04	2.04	1.93	0.99	1.92	1.92	0.84
	Moderately Coarse	–	2.03	2.05	2.04	1.93	1.01	1.88	1.90	0.84
	Finest	–	2.04	2.05	2.04	1.92	1.02	1.84	1.88	0.86
Load NI[1]	Design	2.52	2.89	3.02	2.99	2.99	2.15	3.09	2.93	1.35
	Coarse	2.52	2.89	3.00	3.00	2.97	2.12	3.16	2.95	1.33
	Moderately Coarse	2.52	2.89	3.01	2.99	3.00	2.16	3.12	2.94	1.33
	Finest	2.52	2.90	3.01	2.98	2.98	2.15	3.07	2.92	1.35

(1) The loading NI phase is inclusive of the previous phase.

Table 2.5.4-223
Fracture Density, Hardening Soil, and Lower Bound Sensitivity Analyses

Maximum Settlement (inch)		Nuclear Island	Turbine Building Interior	Turbine Building Exterior	Annex Building	First Bay Building	Radwaste Building	Ancillary Water Tank	Condensate Water Tank	Diesel Generator
Load Other Buildings	Best Estimate	–	2.0	2.0	2.0	1.9	1.0	1.9	1.9	0.9
	Lower Bound	–	2.5	2.5	2.5	2.4	1.3	2.3	2.3	1.2
	Soil Hardening	–	1.9	1.9	1.9	1.8	0.9	1.7	1.7	0.8
	Fractured Zone	–	2.1	2.1	2.1	2.0	1.0	1.9	1.9	0.9
Load NI[1]	Best Estimate	2.5	2.9	3.0	3.0	3.0	2.1	3.1	2.9	1.3
	Lower Bound	3.4	3.7	3.9	3.8	3.9	2.9	3.9	3.8	2.0
	Soil Hardening	2.5	3.0	3.1	3.0	3.0	2.1	3.1	3.0	1.5
	Fractured Zone	2.6	3.0	3.1	3.0	3.0	2.2	3.1	3.0	1.4
Rewatering	Best Estimate	2.1	2.6	2.7	2.7	2.7	1.8	2.7	2.6	1.1
	Lower Bound	2.9	3.3	3.4	3.4	3.4	2.4	3.4	3.3	1.6
	Soil Hardening	2.3	2.8	2.9	2.9	2.9	2.0	2.9	2.8	1.4
	Fractured Zone	2.2	2.6	2.7	2.7	2.7	1.8	2.8	2.6	1.1

[1] The loading NI phase is inclusive of the previous phase.

Table 2.5.4-224
Comparison of Limits of Acceptable Settlement without Additional Evaluation

		Differential Across Nuclear Island Foundation Mat (inch per 50 feet)	Total for Nuclear Island Foundation Mat (inch)	Differential Between Nuclear Island and Turbine Building[1] (inch)	Differential Between Nuclear Island and Other Buildings[1] [2] (inch)
DCD Requirement		0.5	6	3	3
Best Estimate[3]	PLAXIS 3D	0.20	2.5	0.5	1.6
	Hand Calculation	0.21	2.3	0.5	1.9
Lower Bound[3]	PLAXIS 3D	0.23	3.4	0.9	2.2
	Hand Calculation	0.25	3.1	0.8	2.6

[1]   Differential settlement is measured at the center of the NI and the center of adjacent structures.

[2]   Maximum differential settlement occurs between NI and radwaste buildings.

[3]   Settlements presented exclude the rewatering phase.

The following figures will be added in a future revision:

Figure 2.5.4-260 PLAXIS 3D Design Mesh
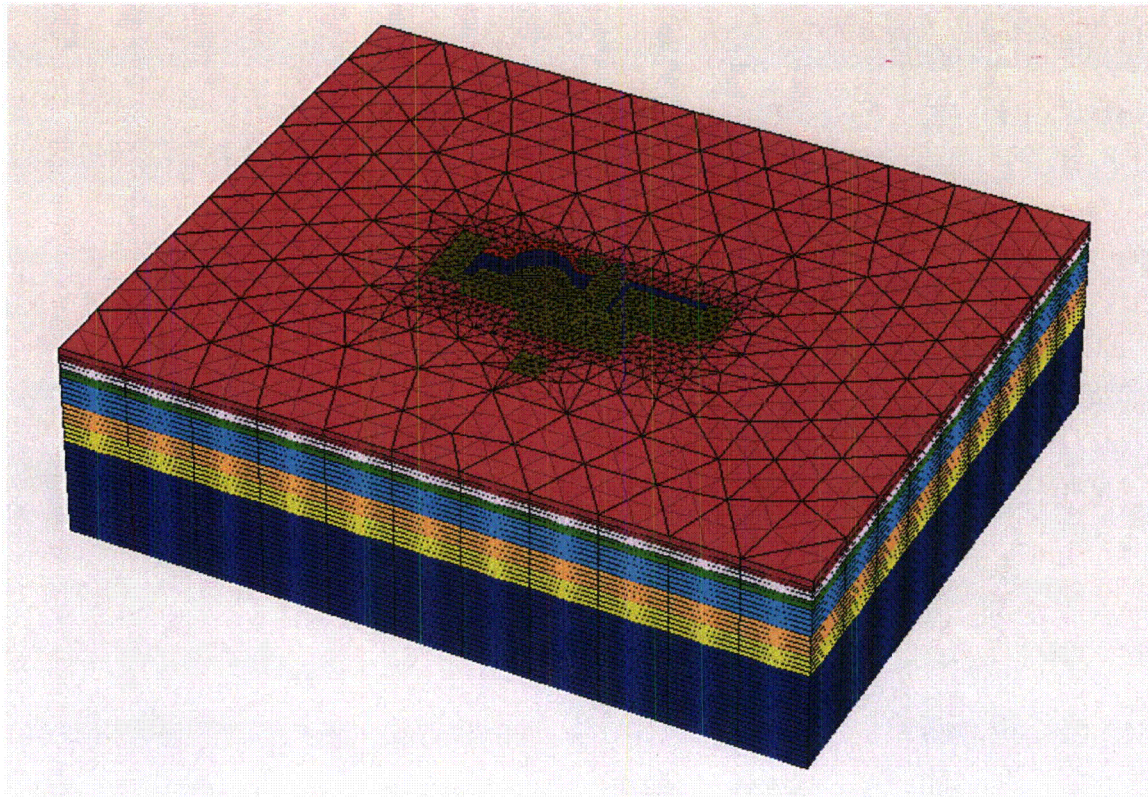
Figure 2.5.4-261 Plot of Soil Hardening Calibration for the Upper Tamiami
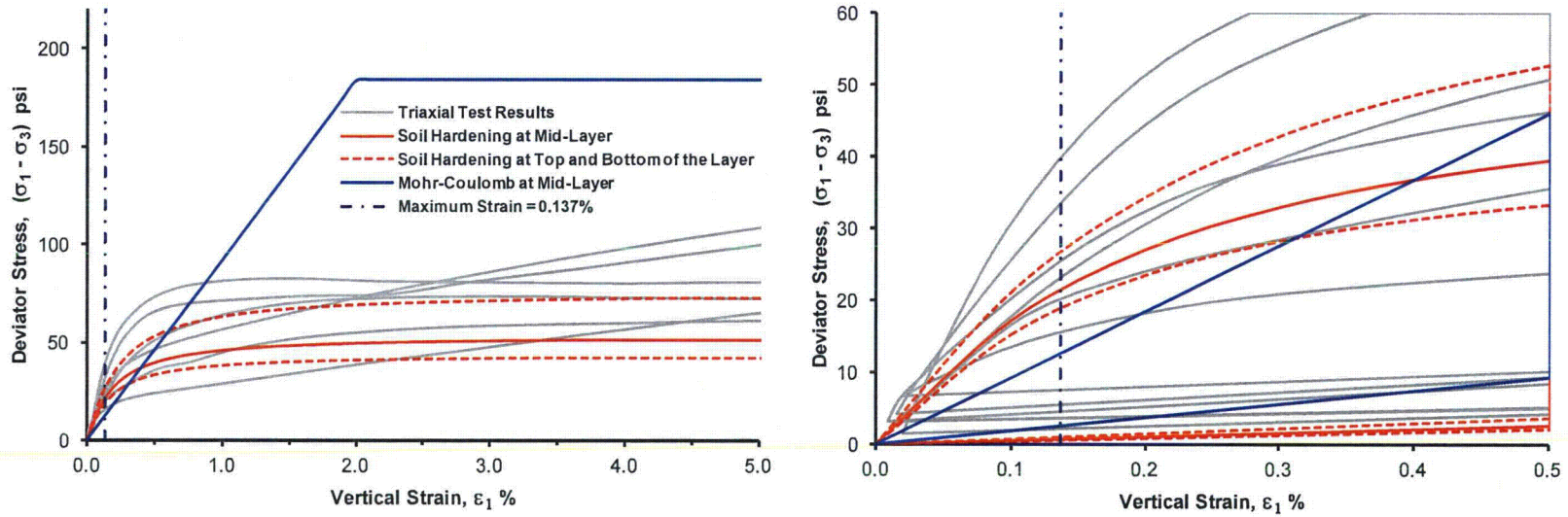
Figure 2.5.4-262 Plot of Soil Hardening Calibration for the Lower Tamiami
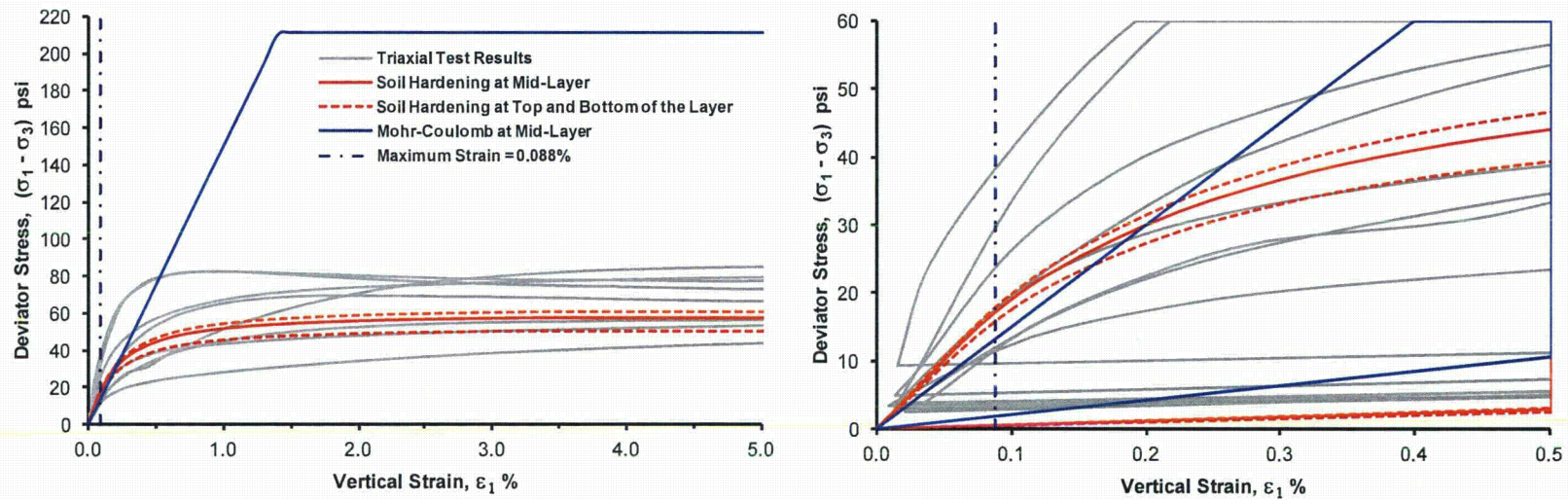
Figure 2.5.4-263 Plot of Soil Hardening Calibration for the Peace River
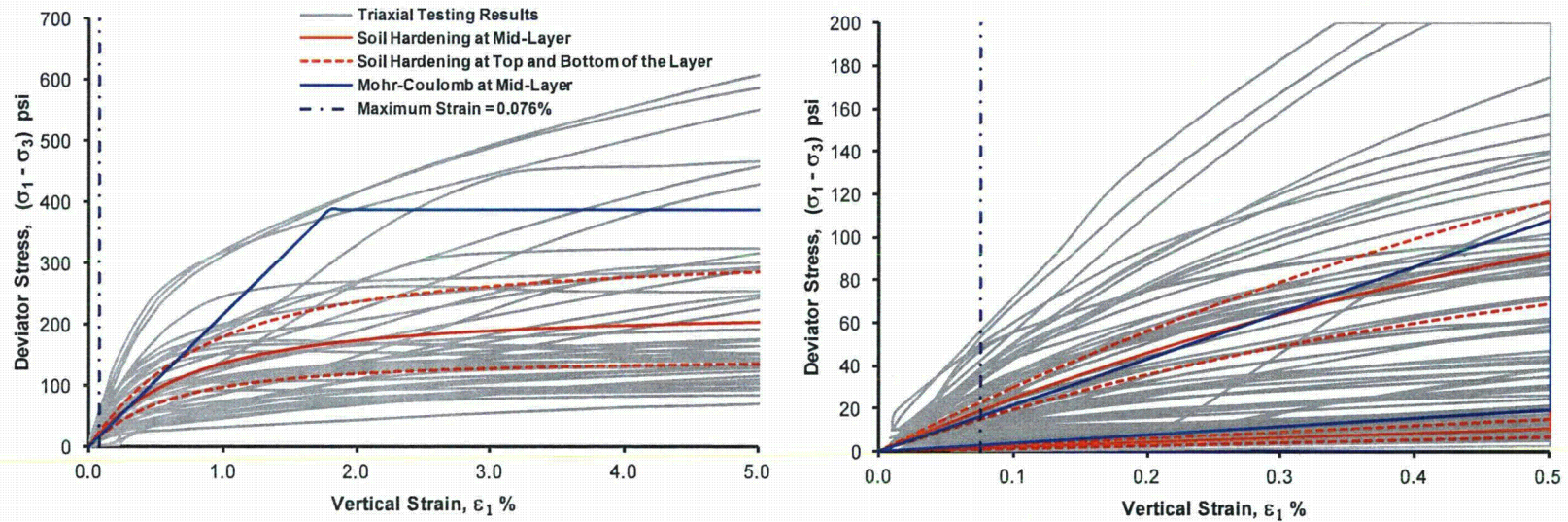
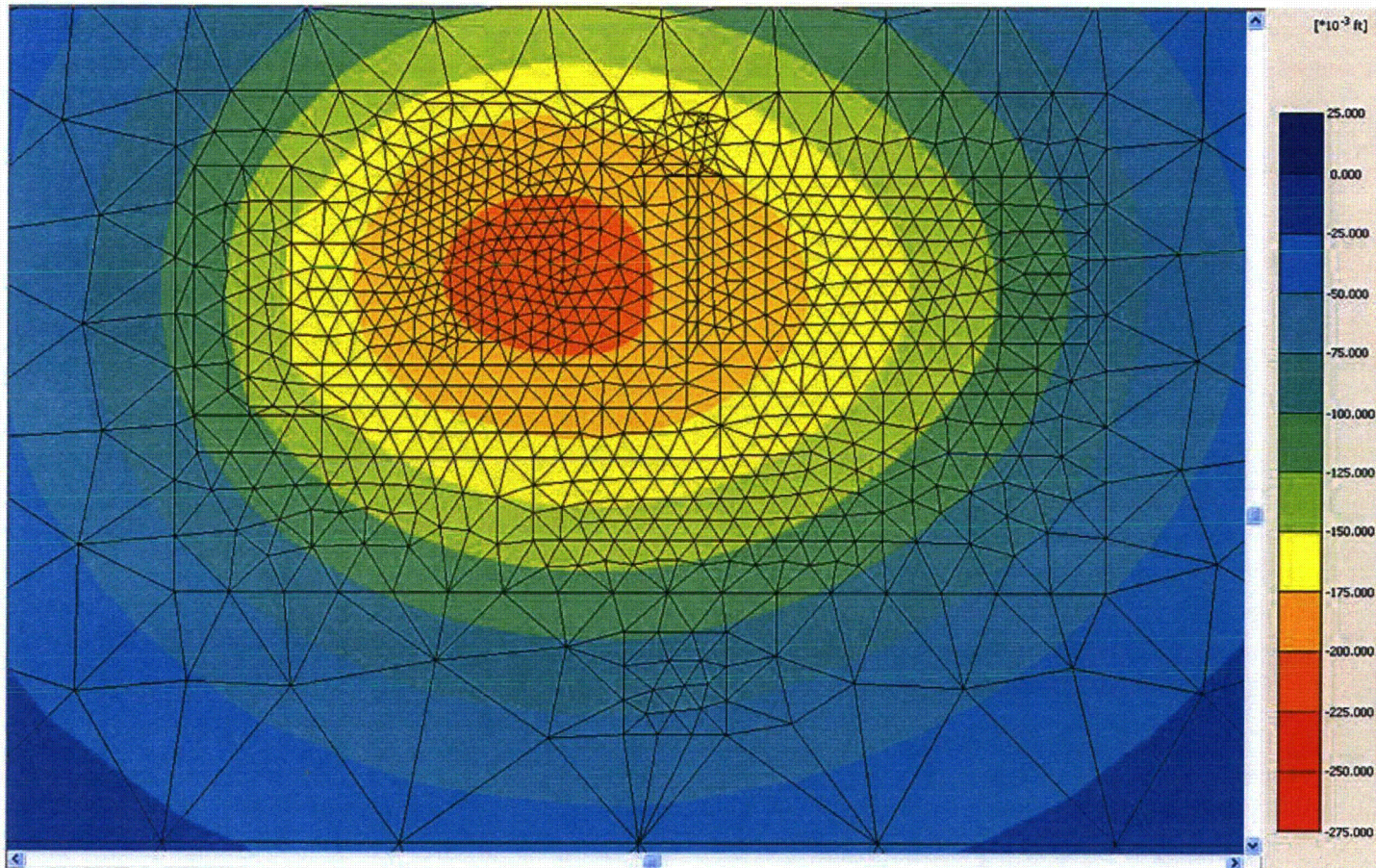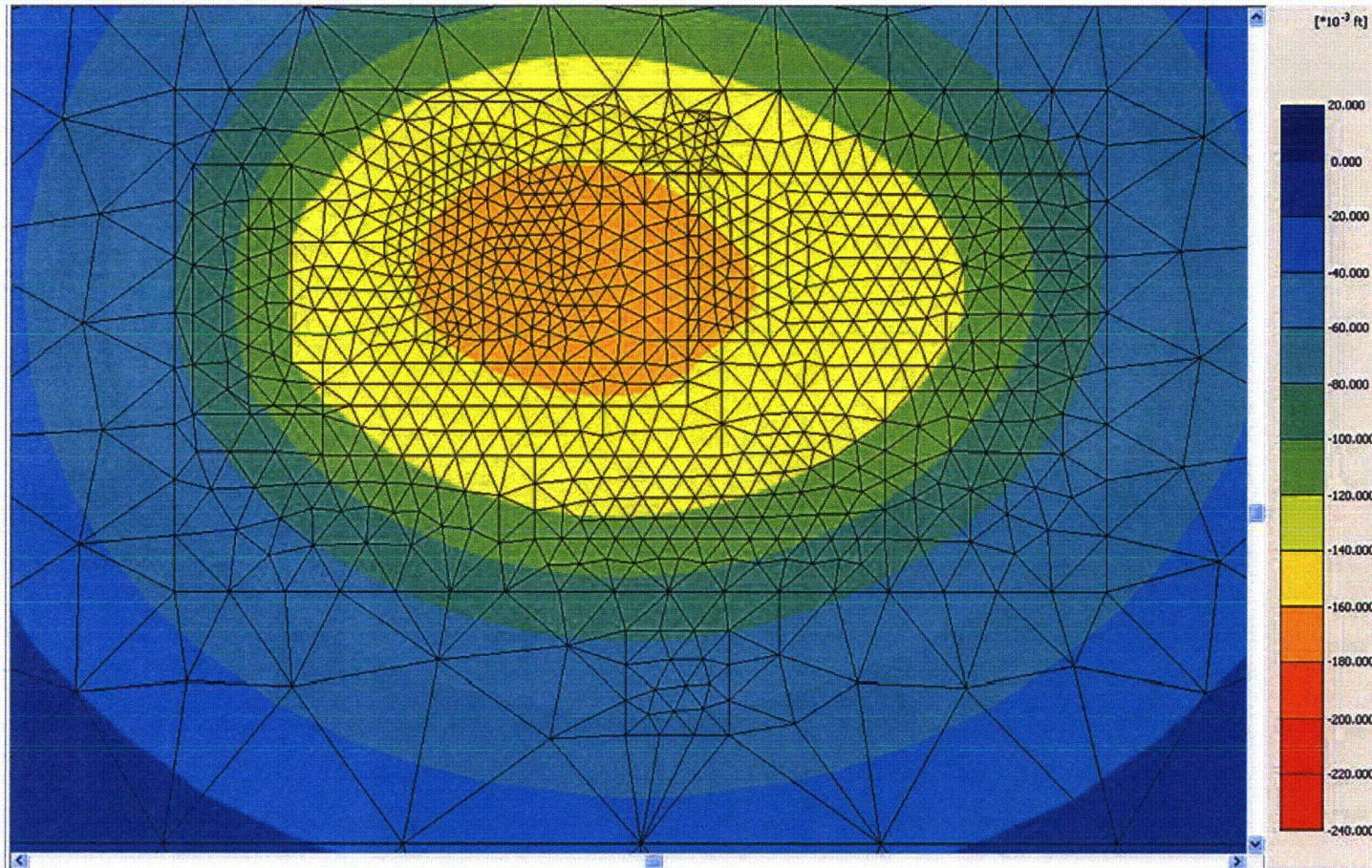**Figure 2.5.4-264 PLAXIS 3D Best Estimate Model Total Settlement After Loading**

Figure 2.5.4-265 PLAXIS 3D Best Estimate Model Total Settlement After Rewatering

ASSOCIATED ENCLOSURES:

None

NRC RAI Letter No. PTN-RAI-LTR-040

SRP Section: 02.05.04 - Stability of Subsurface Materials and Foundations

QUESTIONS from Geosciences and Geotechnical Engineering Branch 1 (RGS1)

NRC RAI Number: 02.05.04-20 (eRAI 6006)

FSAR Subsection 2.5.4.10.3 indicates that the stress distribution used for the settlement calculation was based on Boussinesq distribution. The Boussinesq distribution is based on the assumption that the soil is a homogeneous, linear elastic, isotropic half-space media. In accordance with NUREG-0800, Standard Review Plan, Chapter 2.5.4, "Stability of Subsurface Materials and Foundations," please justify how this method is applicable for the site since a considerable variation in Elastic modulus was reported in the FSAR.

FPL RESPONSE:

The settlement calculation has been revised to use stress distributions appropriate for layered systems. For the nuclear island (NI), a stress distribution from Milovic (Reference 1) for a two-layered system was used with rock (Key Largo and Fort Thompson) as the first layer and soil (upper Tamiami, lower Tamiami, and Peace River) as the second layer. For the remaining buildings (turbine, first bay, annex, and radwaste), a stress distribution from Poulos and Davis (Reference 2) for a three layered system was used with the fill as the first layer; rock (Miami Limestone, Key Largo, and Fort Thompson) as the second layer; and soil (upper Tamiami, lower Tamiami, and Peace River) as the third layer. Since Poulos and Davis (Reference 2) only provides interface stresses and does not provide stresses for the top of the first layer or the bottom of the third layer, linear interpolation is used between the interface stresses from Poulos and Davis (Reference 2) and the top and bottom stresses from the Boussinesq case. It is appropriate to use the top and bottom stresses from Boussinesq because the top stress is equal to the building pressure and the bottom stress is very small due to the large depth. The entire Boussinesq stress distribution is not used in the settlement calculation because it is not appropriate for layered systems as it would yield a highly conservative stress profile. To show how the Boussinesq stress profile results in highly conservative stresses, it is compared to the stress distributions used from References 1 and 2 as well as the results of the finite element method (FEM) model.

Nuclear Island:

The Key Largo Limestone and the Fort Thompson Formation form a stiff upper layer, while the layers below (upper Tamiami, lower Tamiami, and Peace River) are comprised primarily of dense, silty sands. Because of this layering, a typical Boussinesq stress distribution may not provide realistic stress distributions, showing very high settlement in the deep sand layers. Therefore, the stress distribution for a two-layered system from Milovic (Reference 1) was used. This stress distribution is dependent on the stiffness ratio of the upper and lower layers, the thickness of the layers, the area of the building, and the depth of interest. This distribution assumes a Poisson's ratio of 0.15 for the upper layer and 0.45 for the lower layer. The recommended Poisson's ratios for the Key Largo and Fort Thompson formations are 0.3 and 0.34, respectively. The recommended Poisson's ratios for the upper Tamiami, lower Tamiami, and Peace River formations are 0.3, 0.35, and 0.3, respectively. Although, the recommended Poisson's ratios vary from the Poisson's ratios

assumed by Milovic, the stress distribution obtained from Milovic is similar to the stress distribution obtained from the finite element model, indicating that the Poisson's ratio has a secondary effect on the stress distribution. This stress distribution assumes a circular foundation, therefore the radius and diameter of the foundation were found for a circular foundation of equivalent area to the NI.

To obtain this stress distribution, the problem is simplified as shown in Figure 1. The Key Largo and Fort Thompson layers are taken as one layer with a thickness of 80 feet, while the upper Tamiami, lower Tamiami, and Peace River layers are taken as the other layer with a thickness of 339 feet. The concrete is considered rigid with respect to the stiffness of the rock.

Figure 1 Geometry of the Two-Layered System
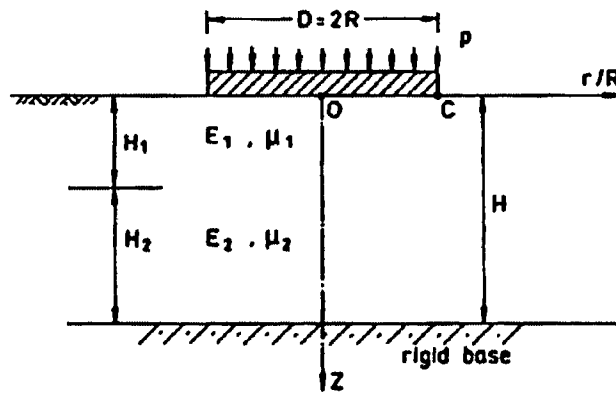
Source: Reference 1

Table 1 shows the Iz coefficients (taken as a percentage of building pressure) for the NI best estimate case.

Table 1
Iz Coefficients for the NI, H/D = 2, H_1 = 0.4D, E_1/E_2 = 10

z/D	Iz r/R = 0	Iz r/R = 1.0
0.05	0.94	0.500
0.15	0.738	0.441
0.25	0.496	0.328
0.35	0.337	0.253
0.45	0.272	0.220
0.55	0.252	0.205
0.65	0.233	0.192
0.75	0.217	0.180
0.85	0.202	0.170
0.95	0.189	0.160
1.1	0.172	0.149
1.3	0.155	0.135
1.5	0.141	0.124
1.7	0.129	0.115
1.9	0.118	0.103

Source: Reference 1

The points shown in Table 1 are plotted and a best-fit curve is generated. This curve is used to define the stress distribution below the NI. For the stress increment beneath the center of the foundation r/R = 0 is used, and for the stress increment beneath the edge of the foundation r/R = 1 is used.

Vertical incremental strains are calculated assuming linear elastic properties. The resulting settlement is obtained by integrating the vertical incremental strains over the soil/rock column.

In addition to the hand calculation described above, stress increments and settlement are modeled using the PLAXIS 3D foundation (PLAXIS 3D). PLAXIS 3D is a finite element method (FEM) based computer code designed for geotechnical analyses. The program calculates displacements with the use of numerical integration methods. In addition to the typical capabilities of a general FEM application for elastic solids, PLAXIS 3D incorporates advanced constitutive models, (stress vs. strain relationship) that are capable of simulating the response of soils to external loading.

The PLAXIS 3D model (Figure 2) includes the shield, auxiliary, radwaste, annex, annex office, and turbine buildings, as well as water tank structures. The PLAXIS 3D model developed uses the same material properties, layering information, building loads, and building areas as the hand calculation. In the PLAXIS 3D model, soil layers are modeled

using elasto-plastic Mohr-Coulomb model, since the strain levels are expected to be low and mostly within the elastic range. Therefore, the numerical finite element solution using PLAXIS 3D is considered to be comparable to the theoretical solution used by the hand calculation. For more information regarding the PLAXIS 3D settlement calculation, see the revised response to RAI 02.05.04-19.

Figure 2 PLAXIS 3D Model
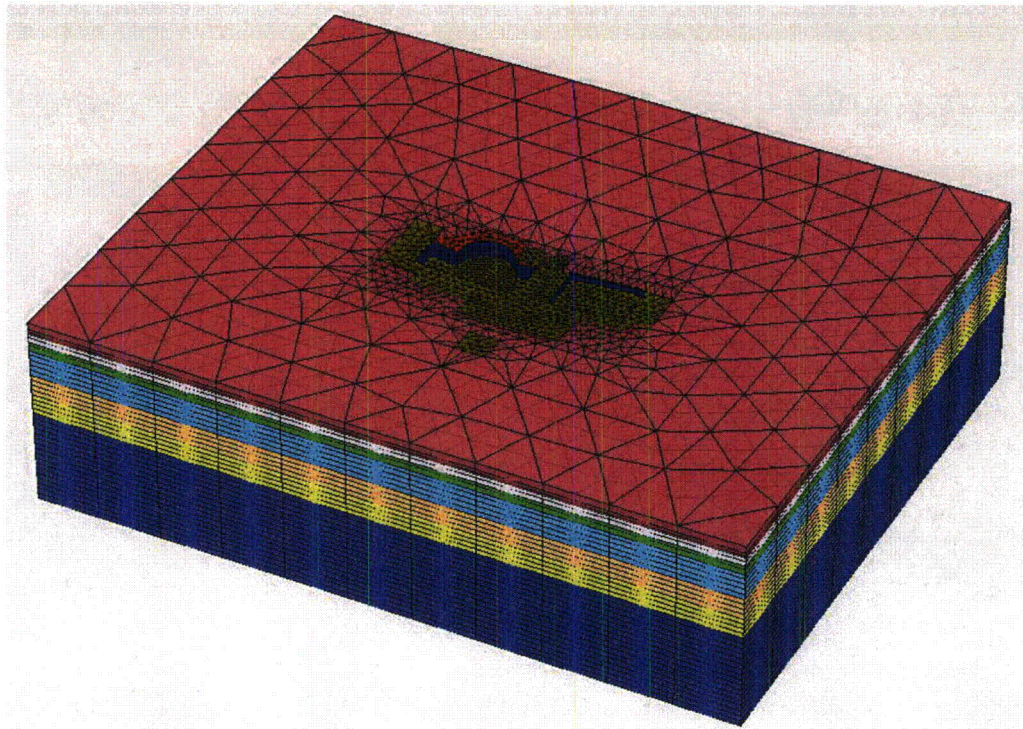
The stress distribution used from Milovic (Reference 1) is compared to the stress distribution provided by PLAXIS 3D as well as Boussinesq as shown in Figure 3.

## Figure 3 Comparison of Stress Distributions
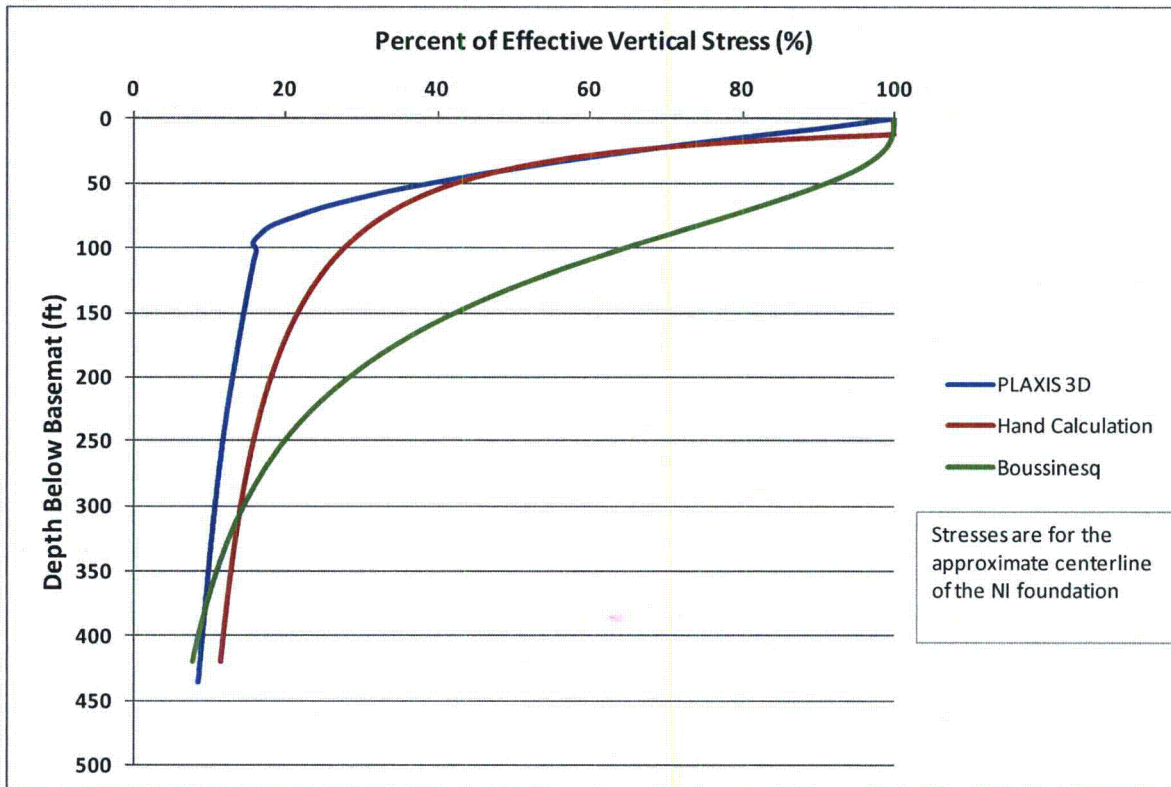
As shown in Figure 3, Boussinesq is highly conservative as it estimates higher stresses in both the rock and soil layers. The stress distribution found by using Reference 1 is similar to but more conservative than the PLAXIS 3D stress distribution. The difference between the PLAXIS 3D and the Milovic stress distributions can be attributed to the fact that PLAXIS 3D estimates the stresses based on all of the soil and rock strata, while the Milovic stress distribution approximates the system as two layers.

Turbine, First Bay, Annex, and Radwaste:

Due to the relatively more compressible fill placed on top of the Miami Limestone beneath the turbine, first bay, annex, and radwaste buildings, a stress distribution from Poulos and Davis (Reference 2) is used that is appropriate for three layered systems. The structural fill is taken as the first layer, the limestone layers (Miami Limestone, Key Largo, and Fort Thompson) are taken as the second layer, and the soils (upper Tamiami, lower Tamiami, and Peace River) are taken as the third layer.

Layer interface stresses are found from Reference 2 for the geometry shown in Figure 4.

Figure 4 Geometry of the Three-Layered System
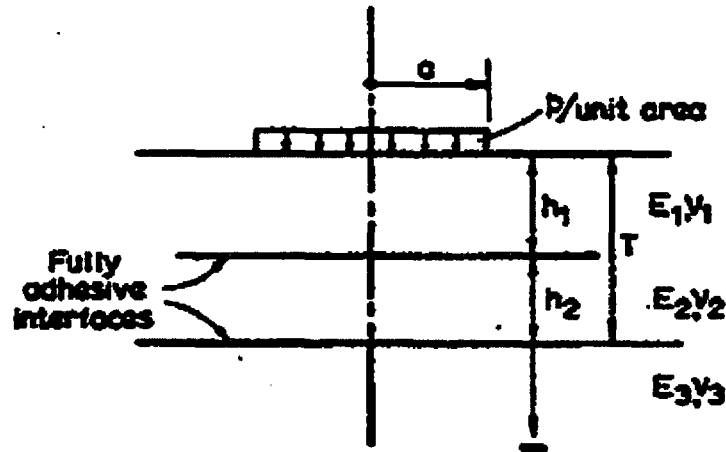
Source: Reference 2, Figure 6.17

Reference 2 provides tables with interface stresses based on the following parameters:

- $k_1 = E_1/E_2$

- $k_2 = E_2/E_3$

- $H = h_1/h_2$

- $a_1 = a/h_2$

The three-layered system has a k_1 value of 0.02. Since interface values are not provided in Poulos and Davis (Reference 2) with k_1 values as low as 0.02, extrapolation was used. Best-fit curves used for extrapolation have R^2 values higher than 0.99, suggesting that extrapolation is appropriate. Table 2 shows the interface stresses from Reference 2 with the values of H and k_2 closest to the parameters for the turbine, first bay, annex, and radwaste buildings (H = 0.25, $k_2 = 20$). For the table of interface stresses presented:

- σ_{z1} is the interface stress (percent of building pressure) at the upper interface

- σ_{z2} is the interface stress (percent of building pressure) at the lower interface

Table 2
Interface Stresses for Three-Layered Systems

$a_1 = 0.4$			$a_1 = 0.8$			$a_1 = 1.6$		
k_1	σ_{z1}	σ_{z2}	k_1	σ_{z1}	σ_{z2}	k_1	σ_{z1}	σ_{z2}
0.2	0.90	0.03	0.2	0.94	0.12	0.2	0.97	0.34
2	0.77	0.03	2	0.93	0.09	2	0.91	0.26
20	0.36	0.02	20	0.69	0.07	20	0.85	0.20
200	0.09	0.01	200	0.23	0.04	200	0.47	0.13

Source: Reference 2

Using extrapolation, the following values were found for $k_1 = 0.02$ (Table 3):

Table 3
Interface Stresses for $k_1 = 0.02$

a_1	σ_{z1}	σ_{z2}
0.4	0.92	0.04
0.8	0.95	0.14
1.6	0.98	0.41

Because a_1 values for the turbine ($a_1 = 1.0$) and radwaste ($a_1 = 0.6$) buildings are in between the a_1 values in Table 3, σ_{z1} and σ_{z2} were found by using interpolation. The interface stresses used for each building are shown in Table 4.

Table 4
Interface Stresses per Building for a Three-Layered System

	Turbine	First Bay	Annex	Radwaste
Upper Interface σz1	0.96	0.92	0.95	0.94
Lower Interface σz2	0.22	0.04	0.14	0.09

Since Poulos and Davis (Reference 2) only provides interface stresses and does not provide stresses for the top of the first layer or the bottom of the third layer, linear interpolation between the interface stresses from Poulos and Davis (Reference 2) and the top and bottom stresses from the Boussinesq case are then used to approximate the stress distribution.

To demonstrate that the stress distribution from Reference 2 is appropriate for the site, the stress distribution of the turbine building is compared to the stress distribution found in PLAXIS 3D as well as Boussinesq (Figure 5).

Figure 5 Comparison of Stress Distributions
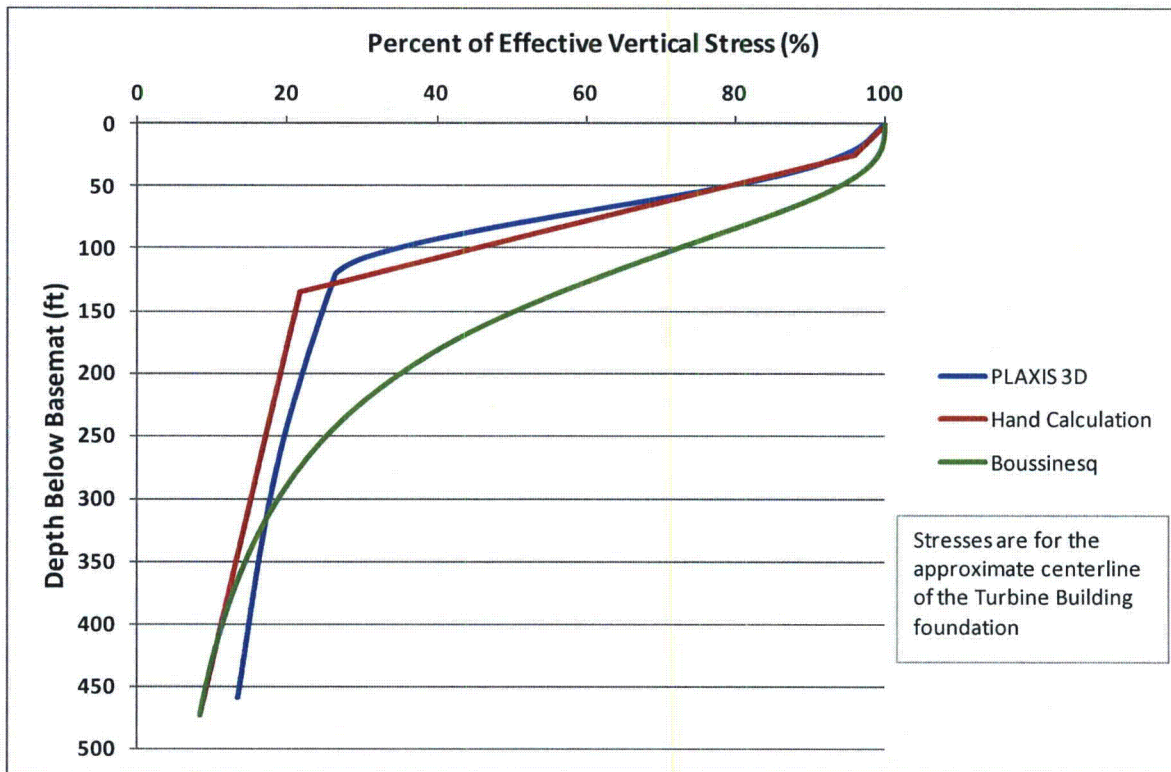
As shown in Figure 5, Boussinesq is highly conservative by estimating higher stresses in both the rock and soil layers. The stress distribution found by using Reference 2 is very similar to the PLAXIS 3D stress distribution demonstrating that it is appropriate for the settlement calculation.

Conclusion:

As shown in Figures 3 and 5, the stress distributions used for the settlement hand calculation from References 1 and 2 are similar to the stress distributions found from the PLAXIS 3D model. The Boussinesq stress distributions are shown to be highly conservative for the site and are not used.

This response is PLANT SPECIFIC.

References:

1.   Milovic, D., *Stresses and Displacements for Shallow Foundations*, Elsevier, 1992.

2.   Poulos, H. G. and E.H. Davis, *Elastic Solutions for Soil and Rock Mechanics*, John Wiley & Sons, Inc., 1974.

ASSOCIATED COLA REVISIONS:

Revisions associated with FSAR Subsection 2.5.4.10.3 and FSAR Table 2.5.4-219 are provided in the revised response to RAI 02.05.04-19.

ASSOCIATED ENCLOSURES:

None

NRC RAI Letter No. PTN-RAI-LTR-040

SRP Section: 02.05.04 - Stability of Subsurface Materials and Foundations

QUESTIONS from Geosciences and Geotechnical Engineering Branch 1 (RGS1)

NRC RAI Number: 02.05.04-22 (eRAI 6006)

The lateral earth pressure diagram shown in Figure 2.5.4-240 shows a plot corresponding to the dynamic lateral earth pressure. The shape of this plot appears to be consistent with the shape for dynamic pressure considering a rigid structural wall (see ASCE 4). In Section 2.5.4.10.4.2 "Seismic Lateral Earth Pressures", the active seismic pressure was computed using the Mononobe- Okabe equation. The last sentence of the section indicates that at-rest pressure as a function of depth for below-grade walls is developed consistent with Reference 277 (ASCE-4) using the design ground motion. It is noted that the pressure developed using the ASCE-4 methodology uses the zpa value from the input motion.

Figure 2.5.2-252 shows the input motion (GMRS) developed for the site, the GMRS is located at Elevation 35. In this Figure the zpa is approximately 0.058g. However, the elevation of the GMRS is considerably lower than the surface of the soils adjacent to the basement walls that are to be evaluated for seismic lateral earth pressure. In accordance with NUREG-0800, Standard Review Plan, Chapter 2.5.4, "Stability of Subsurface Materials and Foundations," please clarify on the definition of the design ground motion, and how that motion is consistent with Appendix S to 10CFR50.

FPL RESPONSE:

FSAR Figure 2.5.2-253 and FSAR Table 2.5.2-228 show the zero period acceleration (zpa) for the GMRS as about 0.058g. This zpa value was not considered appropriate when computing lateral earth pressure because it was developed for El. -35 feet. The design response spectra (DRS) at 5% damping, calculated at the ground surface for the near nuclear island (NI) and far from NI soil sites, were considered appropriate for computing lateral earth pressure, using the envelope of low frequency (LF) and high frequency (HF) acceleration response spectra (ARS) at 10-4 and 10-5 annual probability of exceedance. These ARS envelopes and the DRS are plotted in Figures 1 and 2 for the near NI and far from NI soil sites, respectively. From Figures 1 and 2, the peak ground acceleration at the ground surface is equal to approximately 0.0824g and 0.0806g (DRS at 100 Hertz [Hz]) for the near NI and far from NI soil sites, respectively.

Regarding the computation of active seismic pressure using the Mononobe-Okabe equation, according to Seed and Whitman (FSAR Section 2.5.4 Reference 276), use of horizontal ground acceleration for design at the base level of the wall may result in underestimating the movements. FSAR Section 2.5.4 Reference 276 states that it seems best to use the acceleration at the surface of the backfill, or an average between the surface and the base of the wall. Thus, an acceleration of 0.1g rather than the peak ground acceleration of 0.0824g (near NI) or 0.0806g (far from NI), is conservatively used in the Mononobe-Okabe equation. This value is also consistent with the minimum peak ground acceleration of 0.1g as defined in the Standard Review Plan 3.7.2 Section II.2 and 10 CFR 50 Appendix S.

Similarly, for the computation of at-rest seismic pressure using ASCE 4-98 (FSAR Section 2.5.4 Reference 277), an acceleration of 0.1g, rather than the peak ground acceleration of 0.0824g (near NI) or 0.0806g (far from NI), is conservatively used.

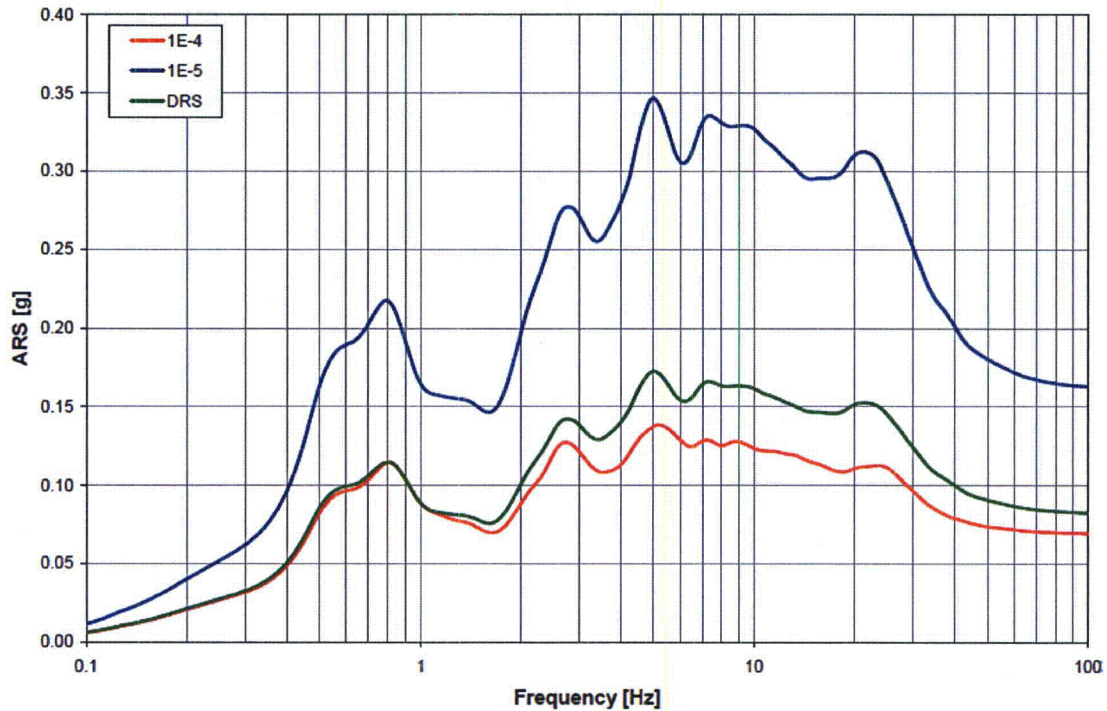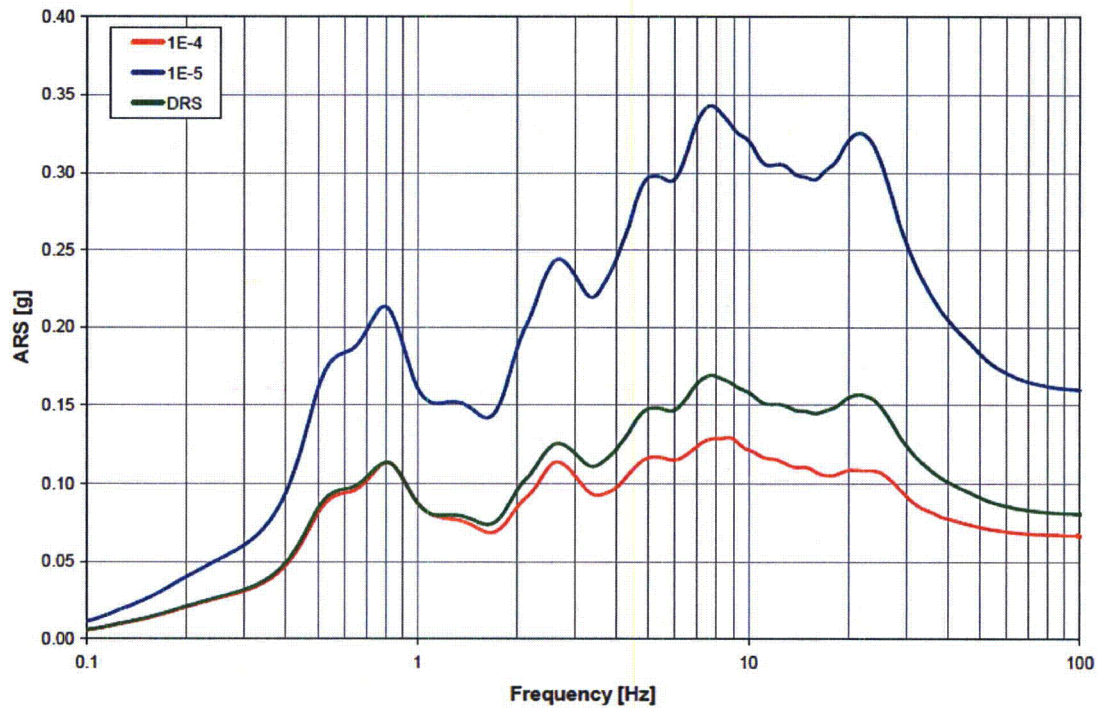**Figure 1 5% Damping ARS at Ground Surface – Near NI, Envelope of LF and HF**

Figure 2 5% Damping ARS at Ground Surface – Far from NI, Envelope of LF and HF

This response is PLANT SPECIFIC.

References:

None

ASSOCIATED COLA REVISIONS:

None

ASSOCIATED ENCLOSURES:

None

NRC RAI Letter No. PTN-RAI-LTR-040

SRP Section: 02.05.04 - Stability of Subsurface Materials and Foundations

QUESTIONS from Geosciences and Geotechnical Engineering Branch 1 (RGS1)

NRC RAI Number: 02.05.04-23 (eRAI 6006)

FSAR Section 2.5.4.10.4.3 states that a surcharge pressure of 500 psf was included when calculating the lateral earth pressures, however the calculation for COL static and seismic lateral earth pressures states that the adjacent building loads and the equipment loads were not considered. In accordance with NUREG-0800, Standard Review Plan, Chapter 2.5.4, "Stability of Subsurface Materials and Foundations," please describe the selection of 500 psf.

FPL RESPONSE:

As indicated in FSAR Subsection 2.5.4.10.4.3, an area-wide surcharge pressure of 500 pounds per square foot (psf) is included in the earth pressure calculations. For the active condition presented in Figure 1 and for the at-rest condition presented in Figure 2, this loading represents the temporary construction loading, and does not include the permanent adjacent building loads. As indicated in FSAR Subsection 2.5.4.10.4.3, the validity of this pressure will be reviewed during the detailed design phase. This temporary loading is conservatively twice the typical design pressure for heavy truck loading (Reference 1).

To address adjacent building loads, an additional case considering a surcharge pressure of 4000 psf is presented in Figures 3 and 4. This surcharge is adopted because it is the highest expected building bearing pressure for the buildings founded on fill around the nuclear island. This pressure will also be reviewed during the detailed design phase.

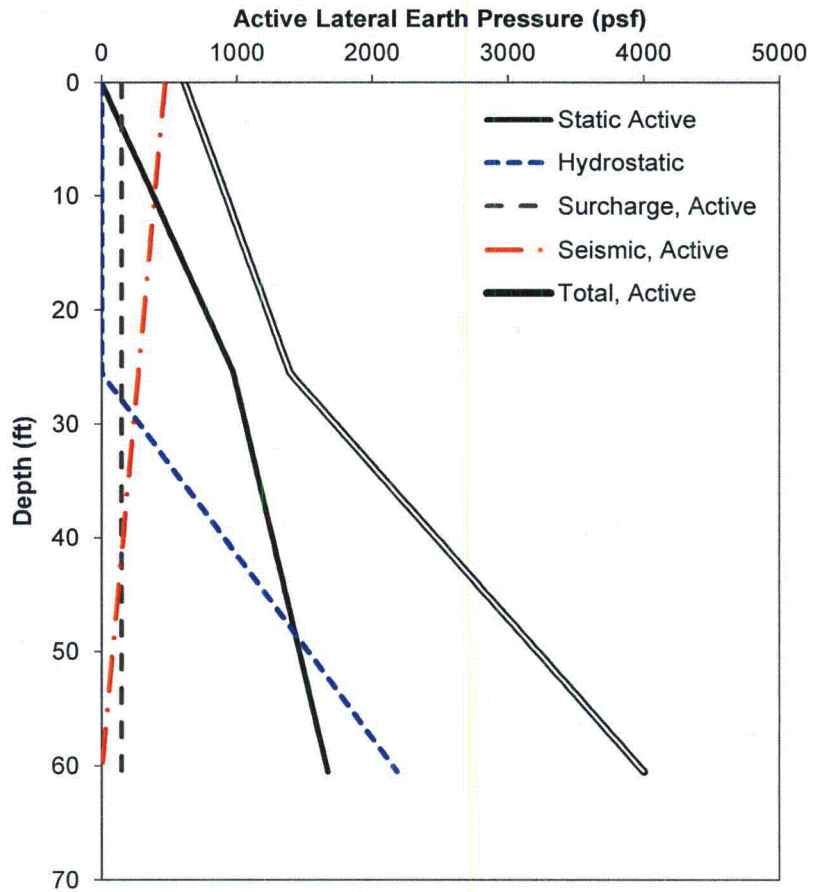## Figure 1 Active Earth Pressure Considering a 500 psf Surcharge on Fill

Active Lateral Earth Pressure (psf)

- Static Active
- Hydrostatic
- Surcharge, Active
- Seismic, Active
- Total, Active

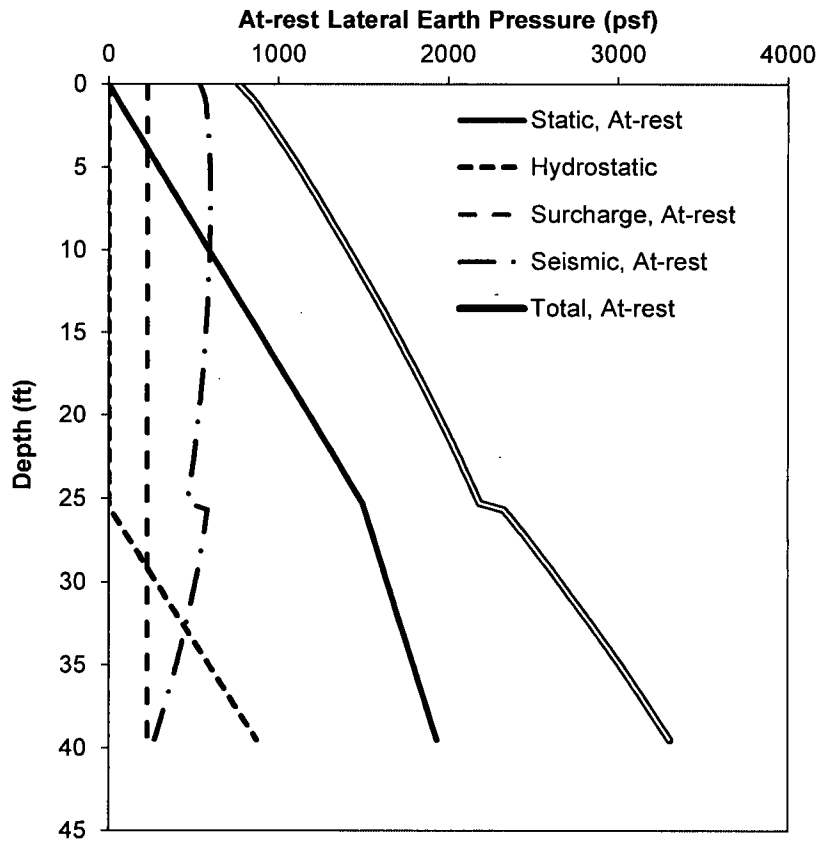## Figure 2 At-Rest Earth Pressures Considering a 500 psf Surcharge on Fill

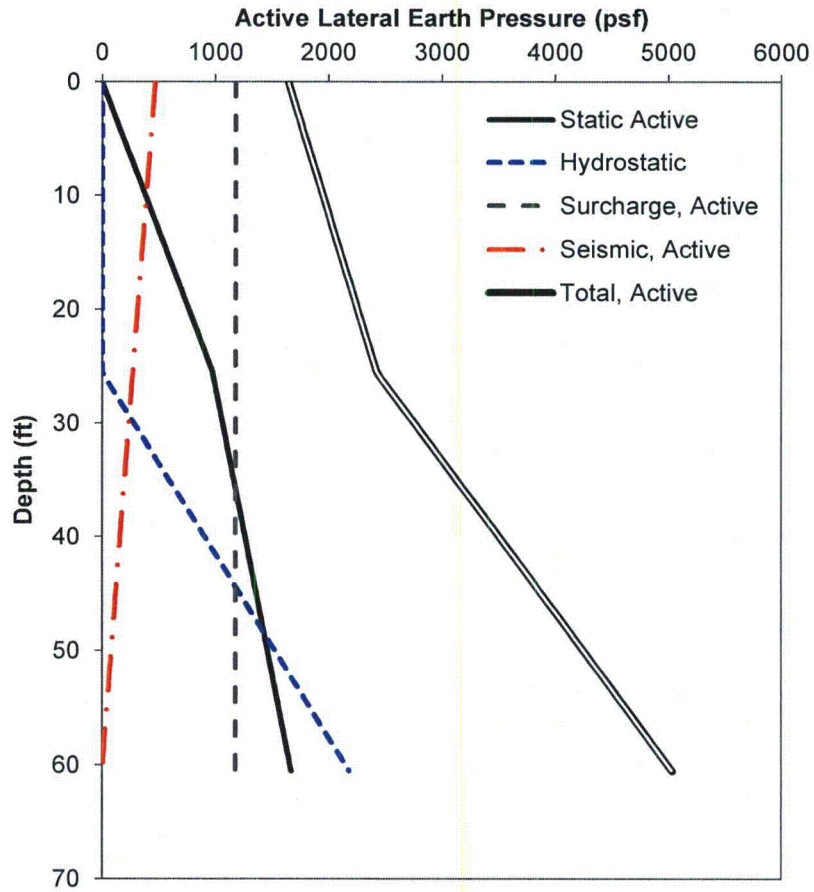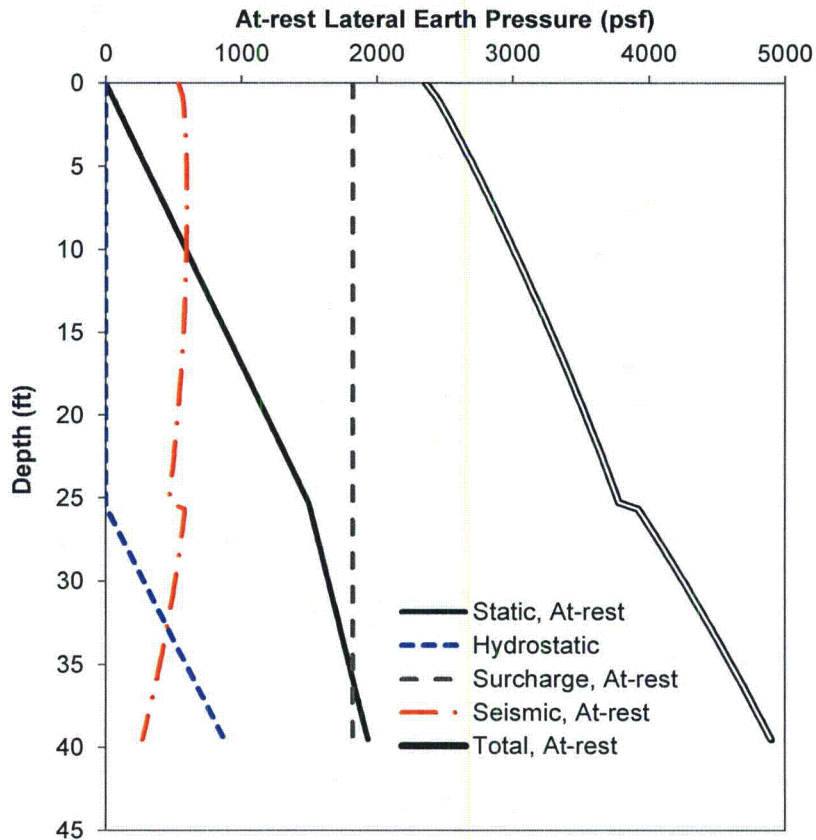### Figure 3 Active Earth Pressure Considering a 4000 psf Surcharge on Fill

Figure 4 At-Rest Earth Pressures Considering a 4000 psf Surcharge on Fill

This response is PLANT SPECIFIC.

References:

1. International Code Council, *2006 International Building Code,* Table 1607.1, Items 24
   and 33, January 2006.

ASSOCIATED COLA REVISIONS:

The last paragraph FSAR Subsection 2.5.4.10.4.3 will be revised in a future revision as
follows:

Note that a-surcharge pressure**s** of 500 psf **and 4000 psf are**is included in the earth
pressure calculations summarized here. The validity of thi**sthese** pressure**s are**is reviewed
during the detailed design phase.

FSAR Subsection 2.5.4.10.4.4, will be revised in a future revision as follows:

Using the relationships outlined above and the compacted limerock fill properties summarized in Table 2.5.4-209, sample earth pressure diagrams are developed. Compacted limerock fill properties (granular soils) used have a unit weight (γ_t) of 130 pcf and a drained friction angle (φ') of 33 degrees (refer to Table 2.5.4-209). These values apply to both structural and general fill. A uUniform surcharge loads of 500 psf **and 4000 psf are**is included.

FSAR Subsection 2.5.4.10.5, will be revised in a future revision as follows:

Recommended diagrams for use in calculating lateral earth pressures against walls are developed based on strata thicknesses and lateral earth pressure coefficients. Figure**s** 2.5.4-239 **(500 psf surcharge) and 2.5.4-252 (4000 psf surcharge)** show**s** the diagram**s** for above grade walls where the walls can rotate or deflect away from the soil mass, known as the active case. This case considered walls extending from the highest finish grade (El. +25.5 feet) to a depth of El. −35 feet, and models active earth pressures on the diaphragm wall during the construction period.

Figure**s** 2.5.4-240 **(500 psf surcharge) and 2.5.4-253 (4000 psf surcharge)** show**s** the pressure diagram**s** for below grade walls where no rotation is possible (at-rest case). This case considers walls from El. +25.5 feet to El. −14 feet, the base of the deepest structure wall.

The last paragraph FSAR Subsection 2.5.4.11 will be revised in a future revision as follows:

Subsection 2.5.4.10 also addresses criteria for static and seismic earth pressure estimation. The calculated lateral earth pressure diagrams shown on Figures 2.5.4-239**,** and 2.5.4-240**, 2.5.4-252, and 2.5.4-253** are best estimates, and thus contain a FOS = 1.0. In the analyses of sliding and overturning due to these lateral loads when the seismic component is included, a FOS = 1.10 is recommended.

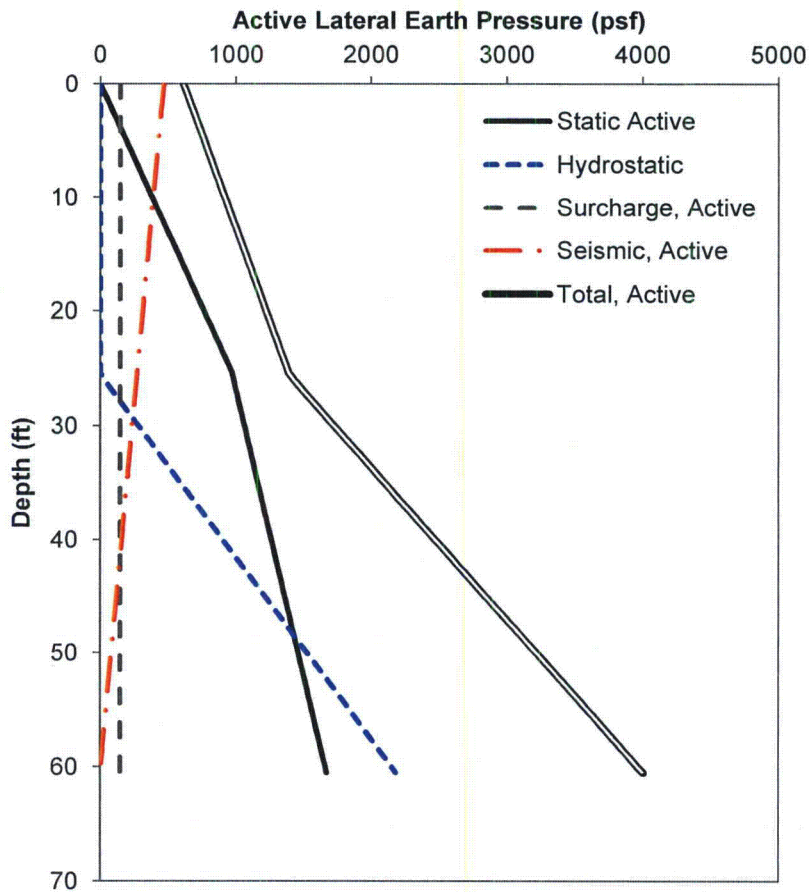FSAR Table 2.5.4-209 will revised in a future revision as follows:

Table 2.5.4-209
Summary of Recommended Geotechnical Engineering Parameters

Stratum[a]	1[a]	2	3	4	5	6	7	8	Fill
Description	Muck	Miami	Key Largo	Ft. Thompson	Upper Tamiami	Lower Tamiami	Peace River	Arcadia	—
Elevation of top of layer (ft)	−1.2	−4.5	−26.7	−49.4	−115.1	−159.0	−215.2	−452.1	—
USCS symbol	ML, MH	GM, GP-GM, SM, SW-SM, SW, SP-SM	Limestone	Limestone	SM, SP-SM	ML	SM	Limestone	—
Total unit weight, γ (pcf)	80	125	136	139	120	120	120	130	130
Natural water content, w, (%)	>80	—	—	—	—	30	—	—	33
Fines content (%)	>60	18	—	—	28	62	16	—	15
Atterberg limits									
Liquid limit, LL	—	—	—	—	—	24	—	—	—
Plastic limit, PL	—	—	—	—	—	20	—	—	—
Plasticity index, PI	—	—	—	—	—	4	—	—	—
SPT N_{60}-value (blows/ft)	~0	20	—	—	40	32	75	—	30
Undrained properties									
Undrained shear strength, s_u (ksf)	—	—	—	—	—	4.0	—	—	—
Internal friction angle, φ, (deg)	—	—	—	—	—	—	—	—	—
Drained properties									
Effective cohesion, c' (ksf)	—	—	—	—	0	1.7	0	—	—
Effective friction angle, φ' (deg)	—	—	—	—	35	20	40	—	33
Average Rock core recovery (%)	—	—	83 to 96	41 to 98	—	—	—	63 to 100	—
Average RQD (%)	—	—	54 to 81	16 to 91	—	—	—	32 to 90	—
Unconfined compressive strength, U (psi)	—	200	1,500	2,000	—	—	—	100	—
Elastic modulus (high strain), E_H	—	630 ksi	2,600 ksi	1,500 ksi	1,500 ksf	2,500 ksf	2,700 ksf	980 ksi	1,100 ksf
Elastic modulus (low strain), E_L	—	950 ksi	2,600 ksi	1,500 ksi	19,700 ksf	25,750 ksf	27,400 ksf	980 ksi	9,100 ksf
Shear modulus (high strain), G_H	—	230 ksi	1,000 ksi	550 ksi	550 ksf	900 ksf	1,000 ksf	360 ksi	420 ksf
Shear modulus (low strain), G_L	—	350 ksi	1,000 ksi	550 ksi	7,300 ksf	9,500 ksf	10,150 ksf	360 ksi	3,500 ksf
Shear wave velocity, V_s, (ft/sec)	—	3,600	5,800	4,250	1,400	1,600	1,650	3,600	860
Compression wave velocity, V_c, (ft/sec)	—	8,000	11,000	8,700	2,900	3,300	3,450	7,850	1,600
Coefficient of sliding	—	0.6	0.7	0.7	0.4	0.3	—	—	0.5
Poisson's ratio, v'	—	0.37	0.31	0.34	0.35	0.35	0.35	0.36	0.3
Static earth pressure coefficients									
Active, K_a	—	0.3	—	—	0.27	0.5	—	—	0.29
At-rest, K_o	—	0.5	—	—	0.5	0.66	—	—	0.46

[a] Properties of Stratum 1 (muck) are not provided as this stratum was removed prior to construction.
    The values tabulated for use as design guideline only. Refer to specific boring logs, CPT logs, and laboratory test results for appropriate modifications at specific design locations.
    USCS = Unified Soil Classification System (ML = silt; MH = silt of high plasticity; GM = silty gravel; GP = poorly graded gravel; SM = silty sand; SW = well graded sand; SP = poorly graded sand).

FSAR Figure 2.5.4-239 will be replaced with the following figure in a future revision:

FSAR Figure 2.5.4-239 ~~Lateral Earth Pressure Diagram: Active Case~~Active Earth Pressure Considering a 500 psf Surcharge on Fill

Data from Table 2.5.4-209 for compacted limerock fill.

FSAR Figure 2.5.4-240 will be replaced with the following figure in a future revision:
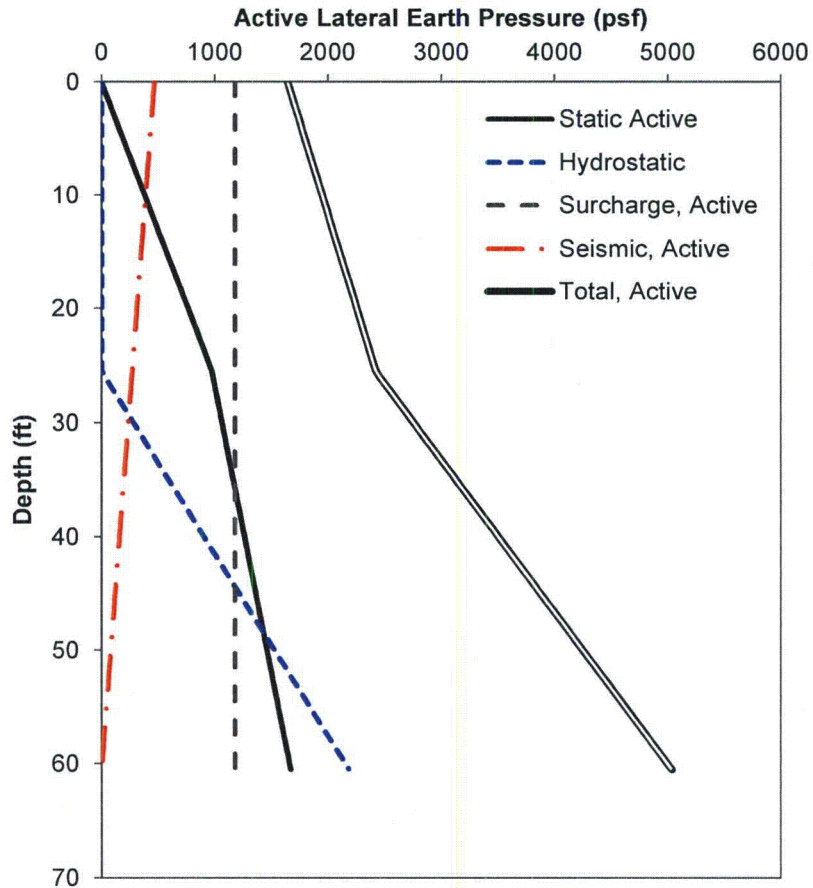
FSAR Figure 2.5.4-240 ~~Lateral Earth Pressure Diagram: At-Rest Case~~At-Rest Earth Pressures Considering a 500 psf Surcharge on Fill
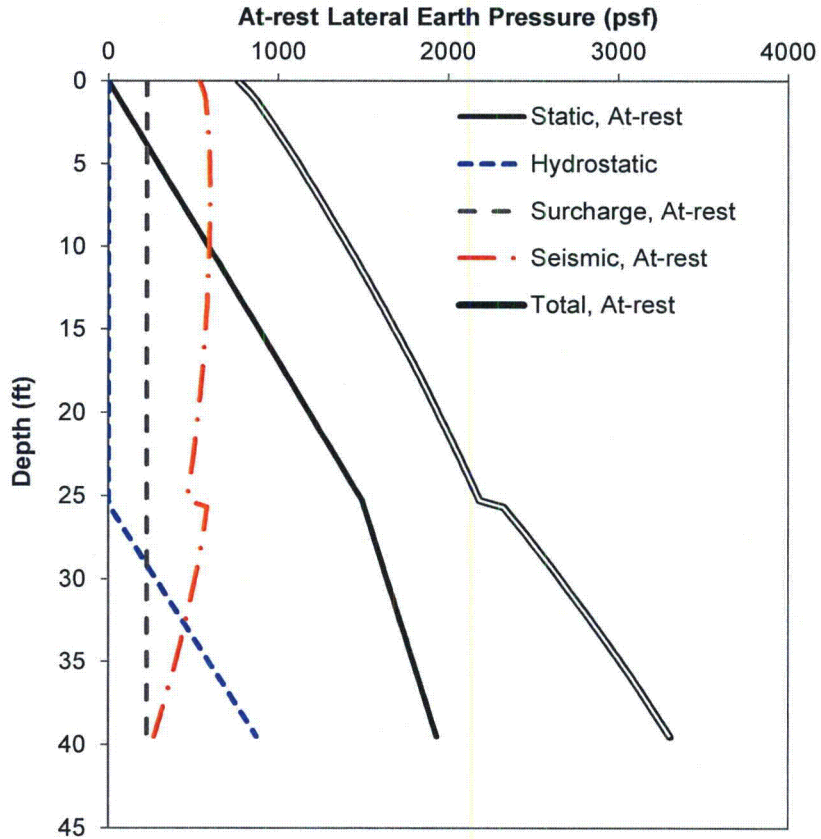
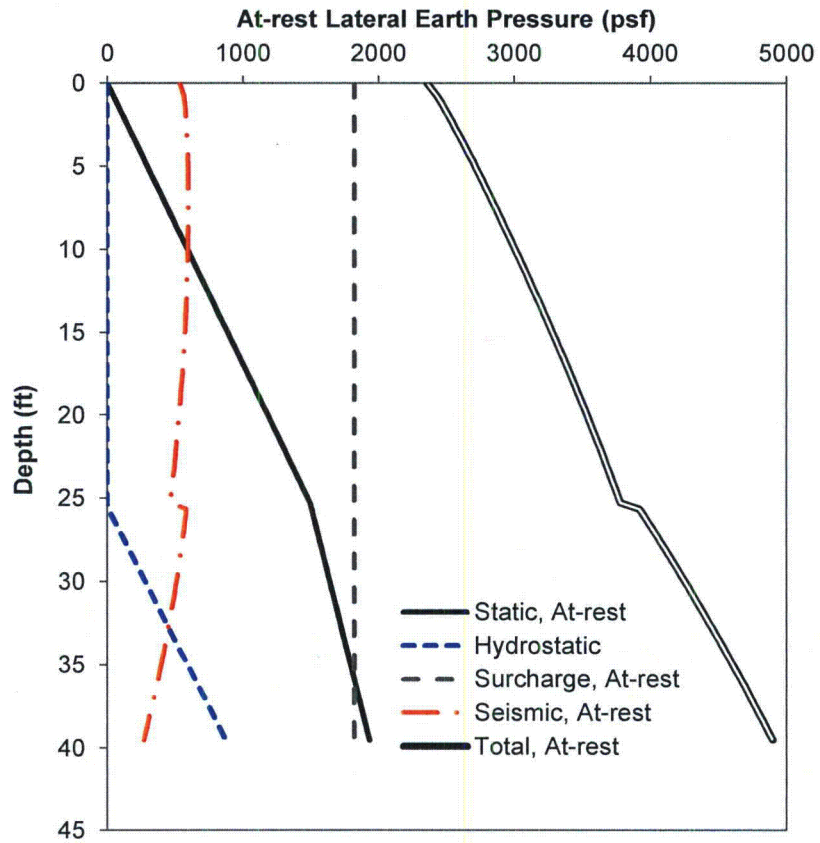Data from Table 2.5.4-209 for compacted limerock fill.

FSAR Figures 2.5.4-252 and 2.5.4-253 will be added in a future revision:

FSAR Figure 2.5.4-252 Active Earth Pressure Considering a 4000 psf Surcharge on Fill

Data from Table 2.5.4-209 for compacted limerock fill.

FSAR Figure 2.5.4-253 At-Rest Earth Pressures Considering a 4000 psf Surcharge on Fill

Data from Table 2.5.4-209 for compacted limerock fill.

ASSOCIATED ENCLOSURES:

None

NRC RAI Letter No. PTN-RAI-LTR-040

SRP Section: 02.05.04 - Stability of Subsurface Materials and Foundations

QUESTIONS from Geosciences and Geotechnical Engineering Branch 1 (RGS1)

NRC RAI Number: 02.05.04-24 (eRAI 6006)

FSAR Section 2.5.4.10.4 states that the active seismic lateral earth pressures were computed using the Mononobe-Okabe methodology and ASCE Standard 4- 98 was used to calculate the at-rest seismic lateral earth pressures. The calculation for COL static and seismic lateral earth pressures calculates at-rest seismic lateral earth pressures using Ostadan method. In accordance with NUREG-0800, Standard Review Plan, Chapter 2.5.4, "Stability of Subsurface Materials and Foundations," please clarify which method was ultimately used for design purposes and provide a justification regarding why ASCE Standard 4-98 was referenced in the FSAR and not Ostadan's method.

FPL RESPONSE:

NUREG-0800 Standard Review Plan, Section 3.8.1 outlines the criteria acceptable to meet the relevant requirements of the U.S. Nuclear Regulatory Commission (NRC) regulations. The subsection titled *Dynamic Soil Pressure* on page 3.8.1-14 of the Standard Review Plan provides that the dynamic lateral earth pressure be calculated in accordance with ASCE 4-98 Section 3.5.3.2.

Seismic active lateral earth pressures were calculated using the Mononobe-Okabe method (FSAR Section 2.5.4 Reference 276) as specified in ASCE 4-98 (FSAR Section 2.5.4 Reference 277) and seismic at-rest lateral earth pressures were calculated using the elastic method as specified in ASCE 4-98 (FSAR Section 2.5.4 Reference 277).

This response is PLANT SPECIFIC.

References:

None

ASSOCIATED COLA REVISIONS:

None

ASSOCIATED ENCLOSURES:

None